Modeling stellar populations in the bulge region

What can we learn from microlensing on Galactic structure

Annie C. Robin

Institut UTINAM, OSU THETA, Université Bourgogne-Franche-Comté, Besançon, France

Outline

- Galactic structure <=> microlensing
- The bulge region complexity
- Besançon galaxy model : a population synthesis approach
- Microlensing in the bulge region : what do we predict ?
- Constraints on Galactic structure, dark matter distribution, and on the IMF from microlensing
- Conclusions

what link between galactic structure and microlensing ?

- Microlensing was first dedicated to detect MACHOS: dark matter distribution in the Milky Way halo (Paczynski 1986, Lukasz Wyrzykowski's tuesday talk)
- Microlensing in the bulge: constraints on mass distribution, wrt light distribution
- Inference on stellar populations, bar shape (angle…), bar mass
- Inference on initial mass function
- Inference on star formation, on planetary formation
- Microlensing with planets => accurate distances => Galactic structure, spiral arms ? (Beaulieu tuesday talk)

Galaxy modeling

- Modeling helps the understanding
- Confronting a scenario with observations
- Confronting various observational constraints to a unique scheme:
  - light distribution (various wavelengths),
  - star count distributions, by types, gravities, metallicities
  - dynamical mass estimates from kinematics and star counts
  - microlensing
- Towards a unique scenario that explain most observational constraints

The bulge region complexity

Due to

- Our view from the outer Galactic plane
- High interstellar extinction
- Superposition of different populations

Extinction !

- Needed to be taken into account for understanding the bulge stellar populations
- Need distances to correct for extinction
- Several attempts to determine 3D extinction distribution
- Examples:
    - Drimmel & Spergel 2001
    - Marshall et al 2006
    - Lallement et al 2015
    - Green et al 2015

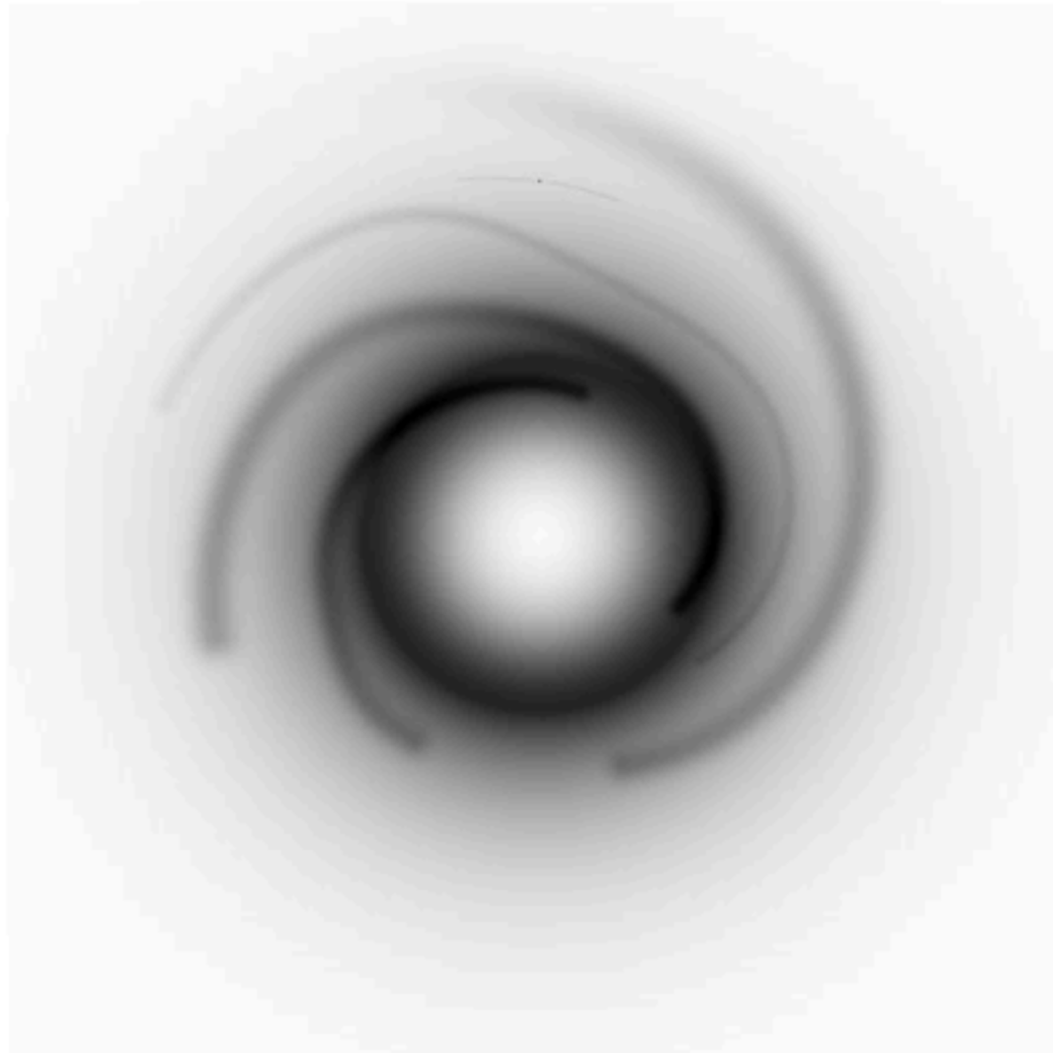

FIG. 13.—Surface density map of the dust, as inferred from the dust density model. Small black dot (*upper center*) shows the position of the Sun, which nearly lies on a small local feature, known as the Orion arm. Arms are incomplete on the side opposite the Sun owing to incomplete H II data.

Drimmel and Spergel, 2001,
Fit a multi-component model (dust+stars) to integrated light in NIR and FIR

Interstellar Extinction

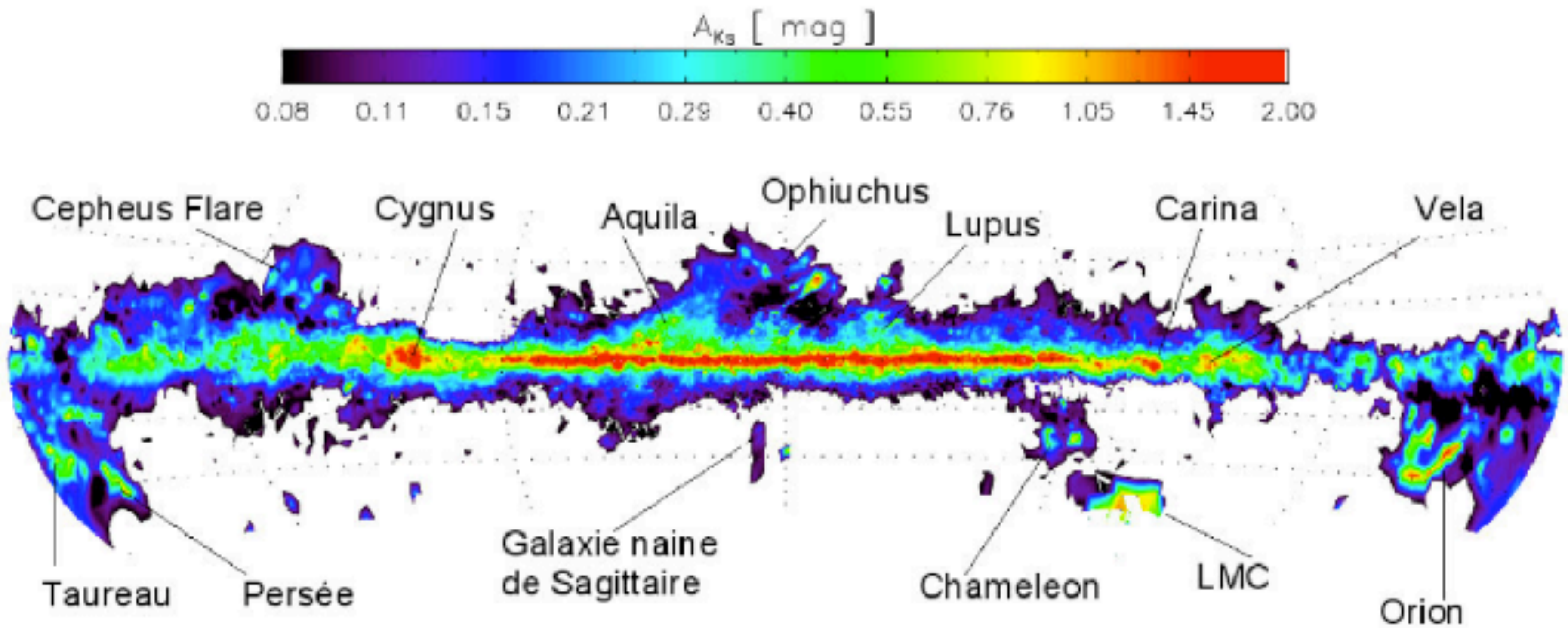

3D extinction map of the Milky Way
(Marshall et al., 2006)

- Correction for stellar model
- Galactic structure
- Used for large range of science in the literature

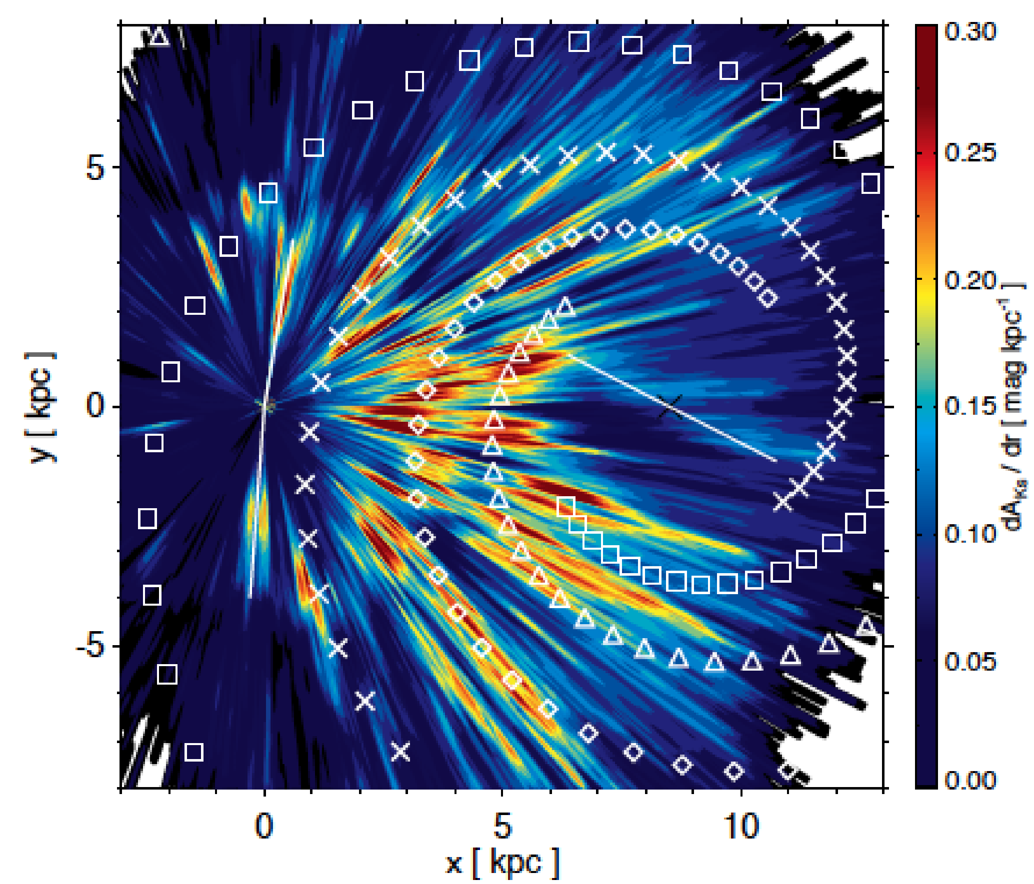

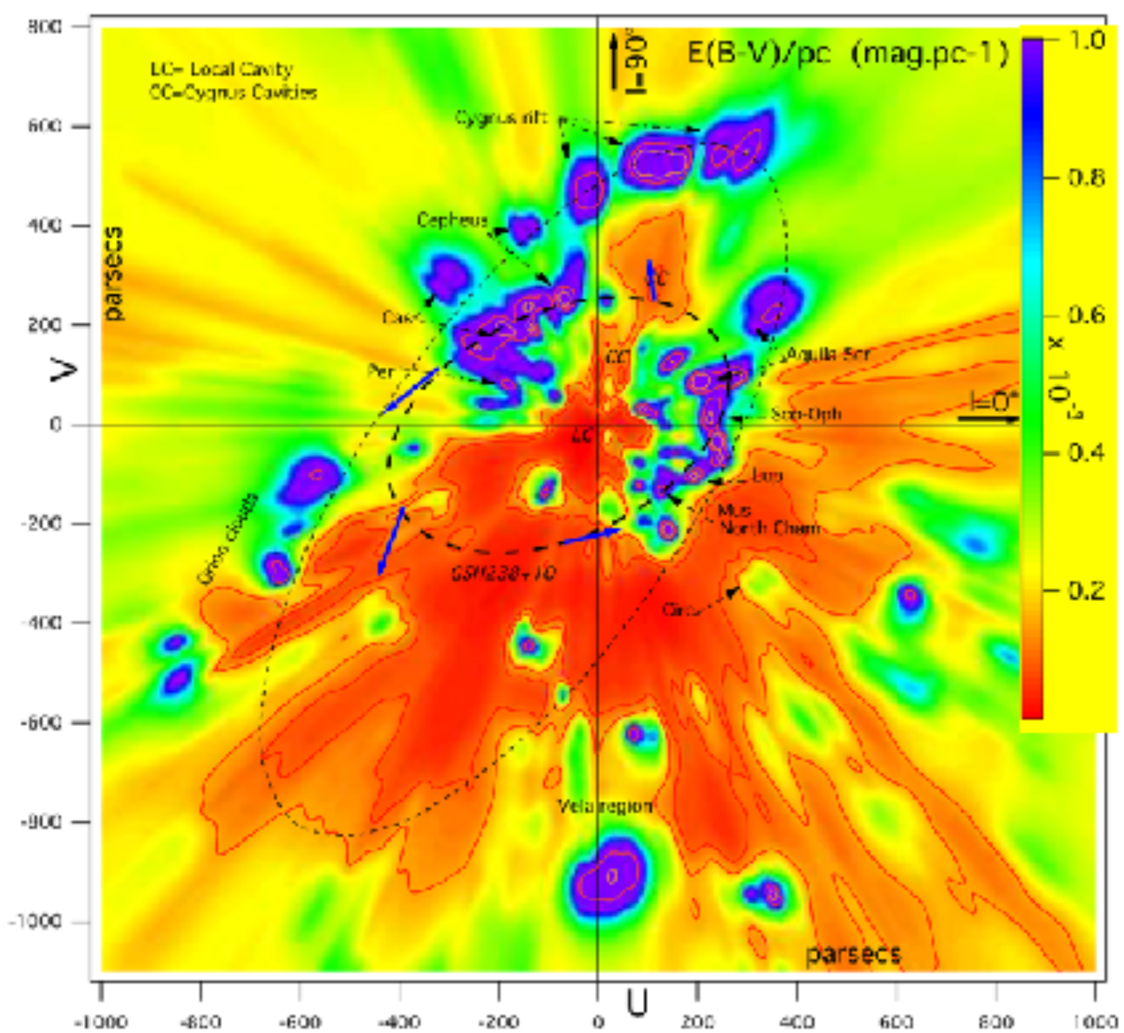

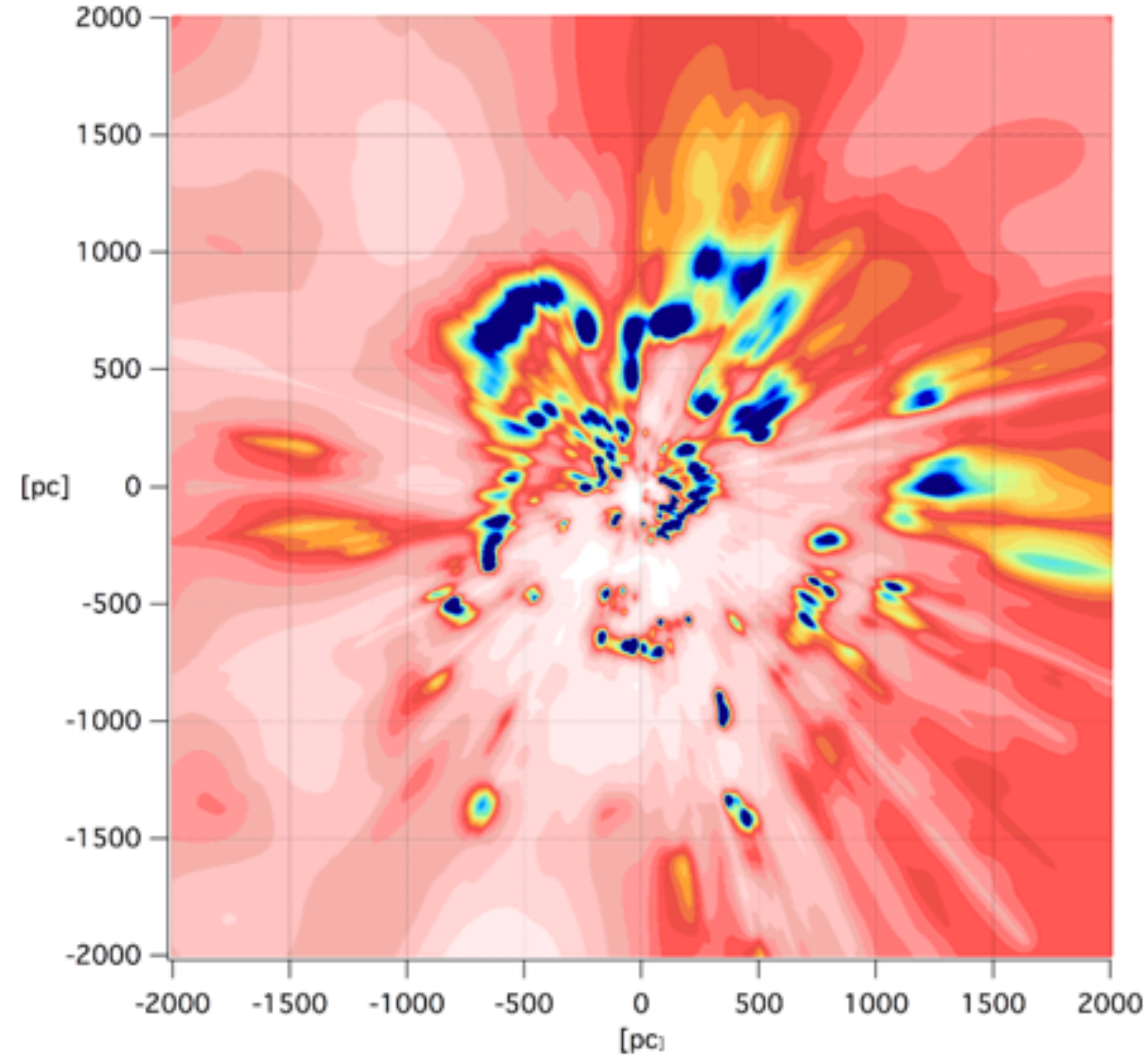

Lallement et al (2014): local map from individual E(B-V) inversion method

Capitanio et al (2017): New map up to 2 kpc

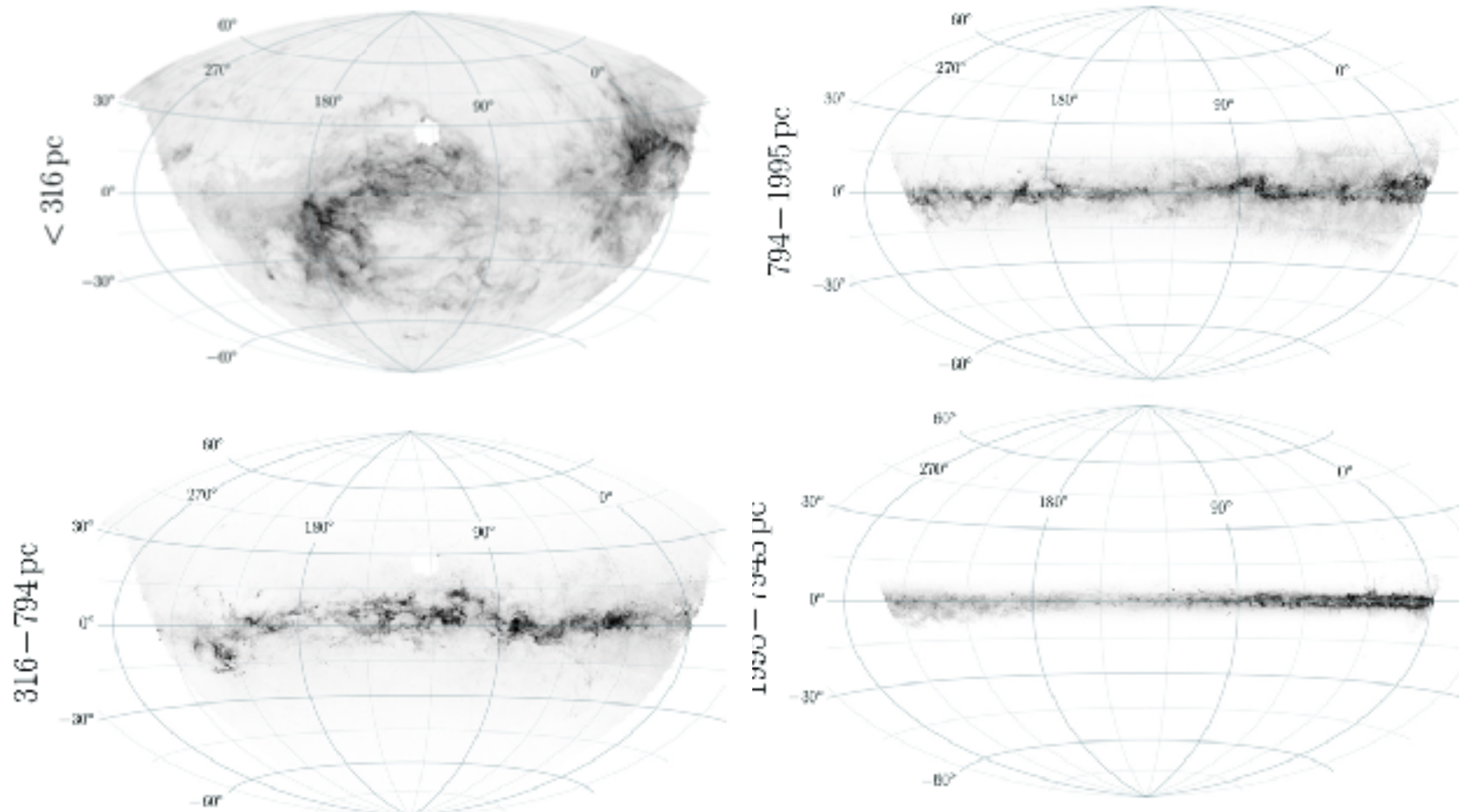

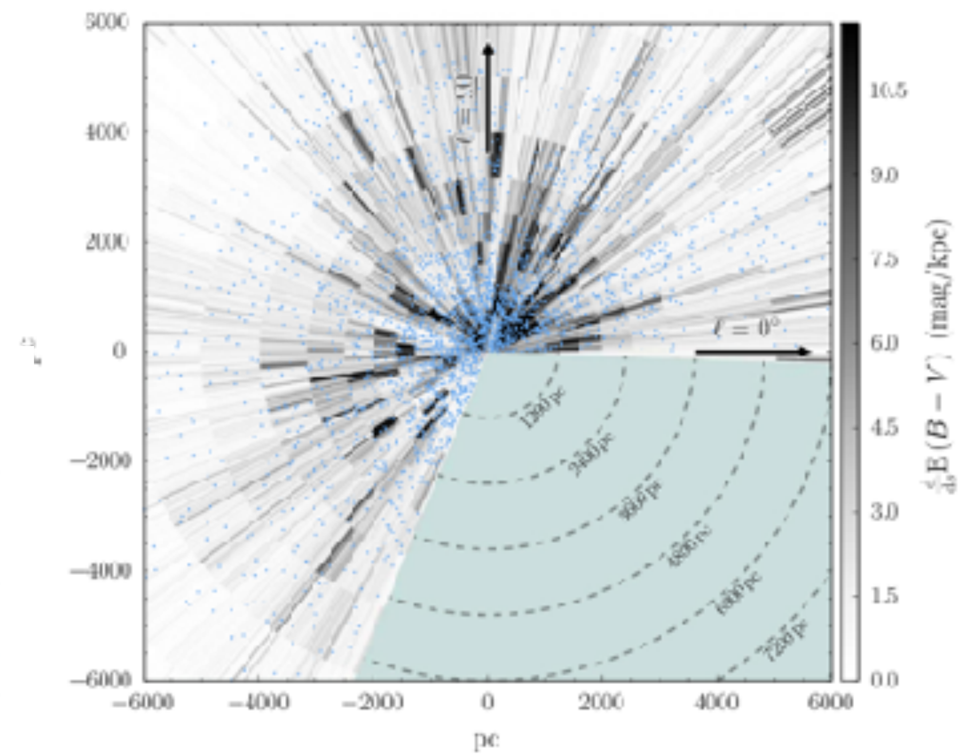

dust in-plane (X,Y)

Green et al (2016)
From Pan-Starrs photometry and Markov Chain Bayesian fitting method

Extinction

- S
- N
- C
  P
- S
  (c
  M

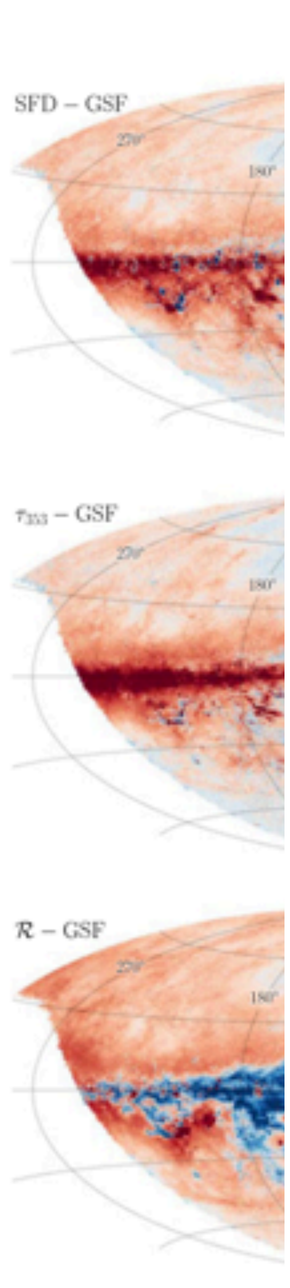

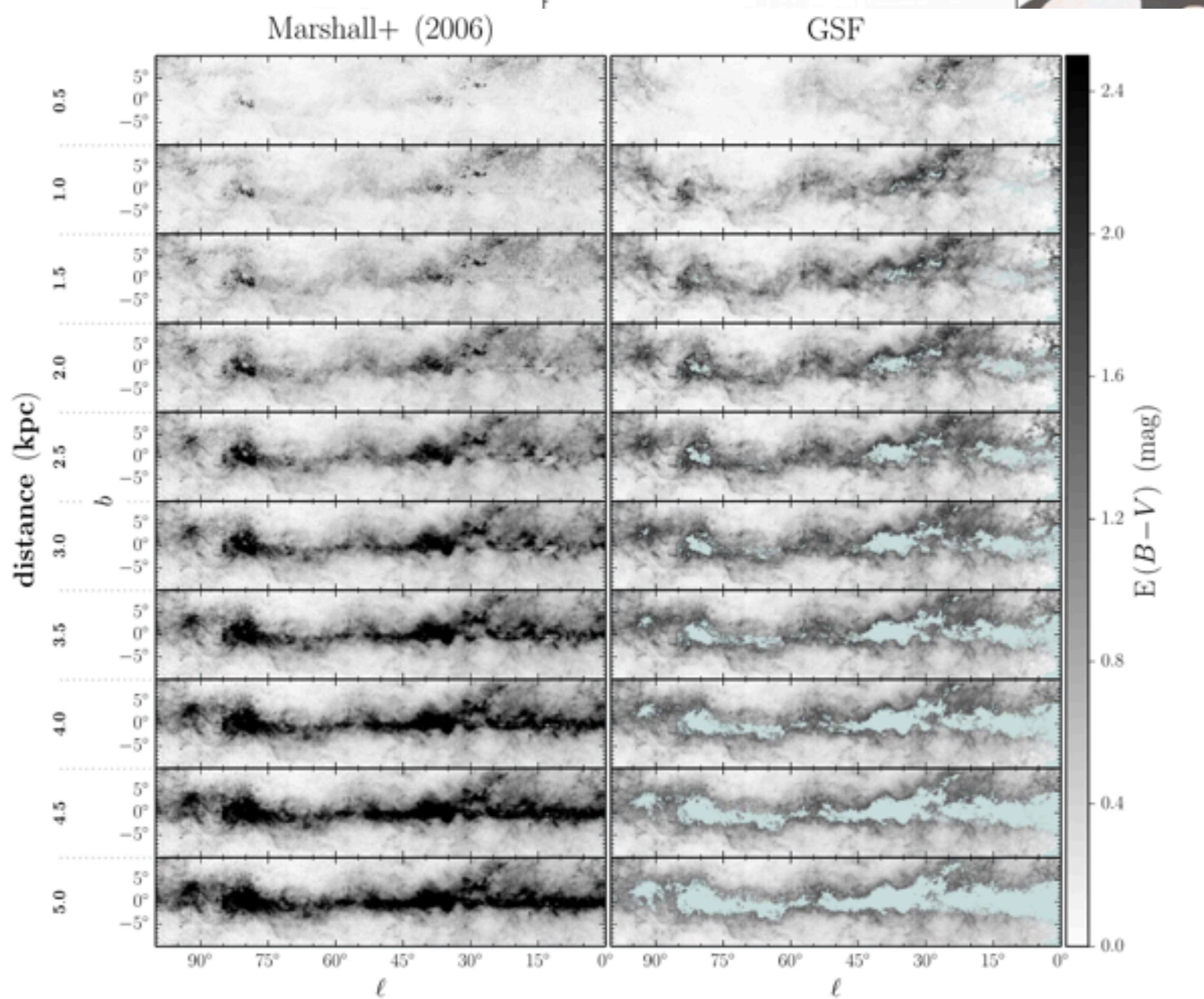

Figure 13. Comparison of the median cumulative reddening out to increasing distances in the Marshall map (left panel) and our map (right panel). Regions beyond the maximum reliable distance in our map are masked out in blue in the right panel. At large distances, the two maps agree qualitatively, with the masked regions in our map corresponding to the most heavily obscured regions in the Marshall et al. (2006) map. The Marshall map has greater depth, but lower angular resolution, and lower distance resolution in the nearest two to three kiloparsecs.

Figure 12. Comparison of … map (denoted by $\mathcal{R}$). The left p… right show the histogram of the … e put the $\tau_{353\,\mathrm{GHz}}$-based reddeni… ening estimates. In the bottom t… errors should be uncorrelated with those of the quantities along the y-axis. An inset in the top-right panel shows the regions that are masked in this analysis. The detailed behavior of the residuals, particularly at large reddenings, depends on which regions are masked, indicating that there are systematic differences in the residuals between our reddening map and emission-based map in different regions of the sky.

Stellar populations in the bulge region

- Denomination : bar versus bulge ?
- Stellar populations of controversial origin :
    - **Bar**: from instability in the disc, complex orbits
    - **Classical bulge**: spheroidal structure, old, radial orbits
    - **Mergers**
- Several scenarios can be present
- Contributions of **other populations** (thin disc, thick disc and halo) can be significant

X-shape or boxy shape ?

- **Apparent X-shape (Ness & Lang, 2016 from WISE data)**
- X-shape from double-clump observations
- Young F-dwarfs (< 5 Gyr): no X-shape (Lopez-Corredoira)
- Old (RR-Lyr, Miras) > 10 Gyr: No X-shape

Fig. 3.— The WISE W1 and W2 image fit by a simple exponential disk model, making the X structure more apparent. Top-left: Data. Top-middle: Data, ma the top and bottom 5% of pixels based on W1−W2 color, as well as pixels with negative flux. The diagonal structure at the top of the image is due to scatte from the Moon in the unWISE coadds. Top-right: Exponential disk model fit. Bottom-left: Residuals (data minus model). Bottom-middle: Masked residuals. right: 50-pixel (~1.7○) median filter of masked residuals (median of unmasked pixels).

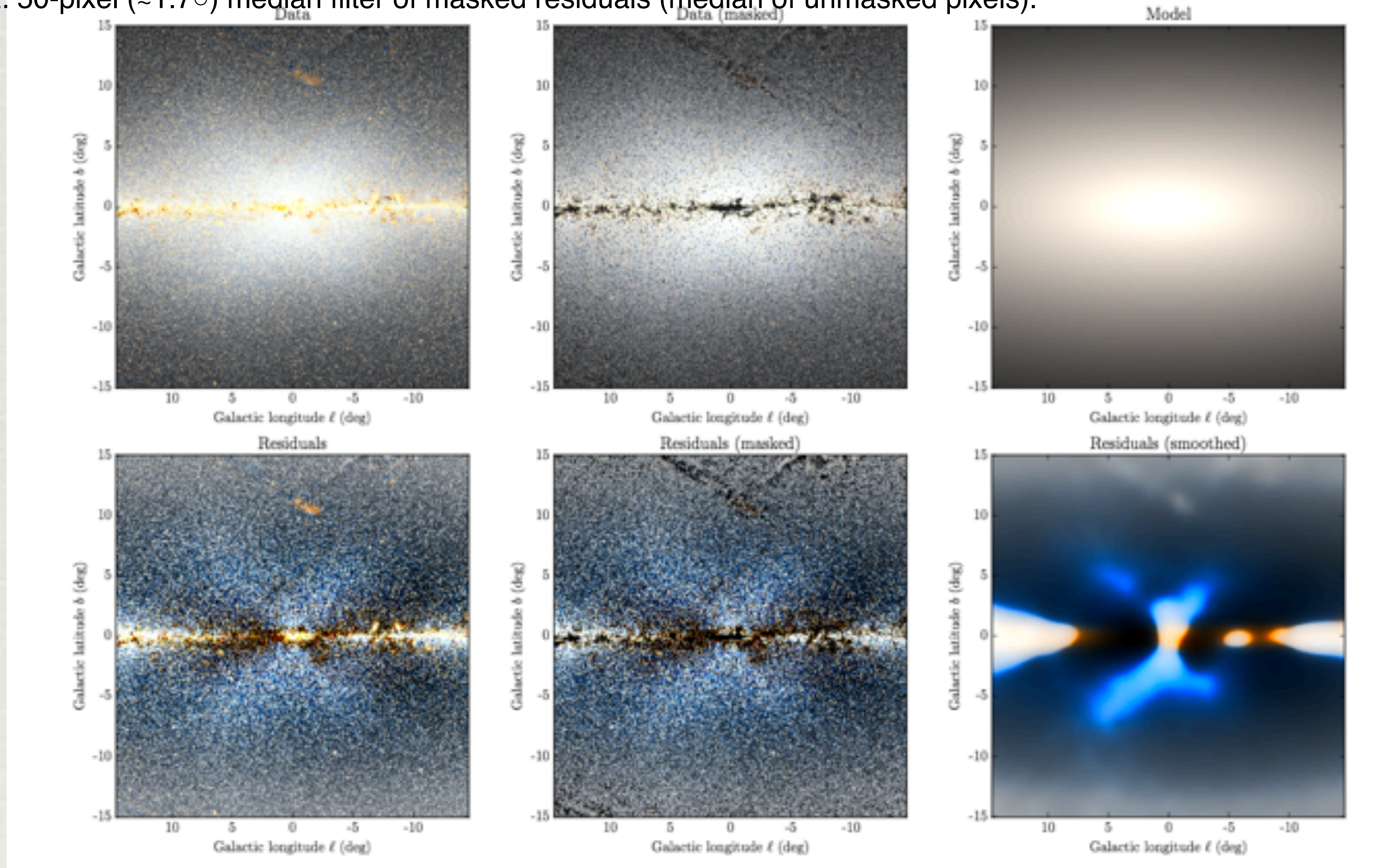

Boxy shape !

Ness & Lang, 2016
https://arxiv.org/pdf/1603.00026.pdf

X-shape or boxy shape ?

- Apparent X-shape (Ness & Lang, 2016 from WISE data): this is boxy !
- **X-shape from double-clump observations**
- Young F-dwarfs (< 5 Gyr): no X-shape (Lopez-Corredoira)
- Old (RR-Lyr, Miras) > 10 Gyr: No X-shape
- Clue for age of the bar buckling

WFI (ESO 2.2m) l=0° b=-6°   OGLE

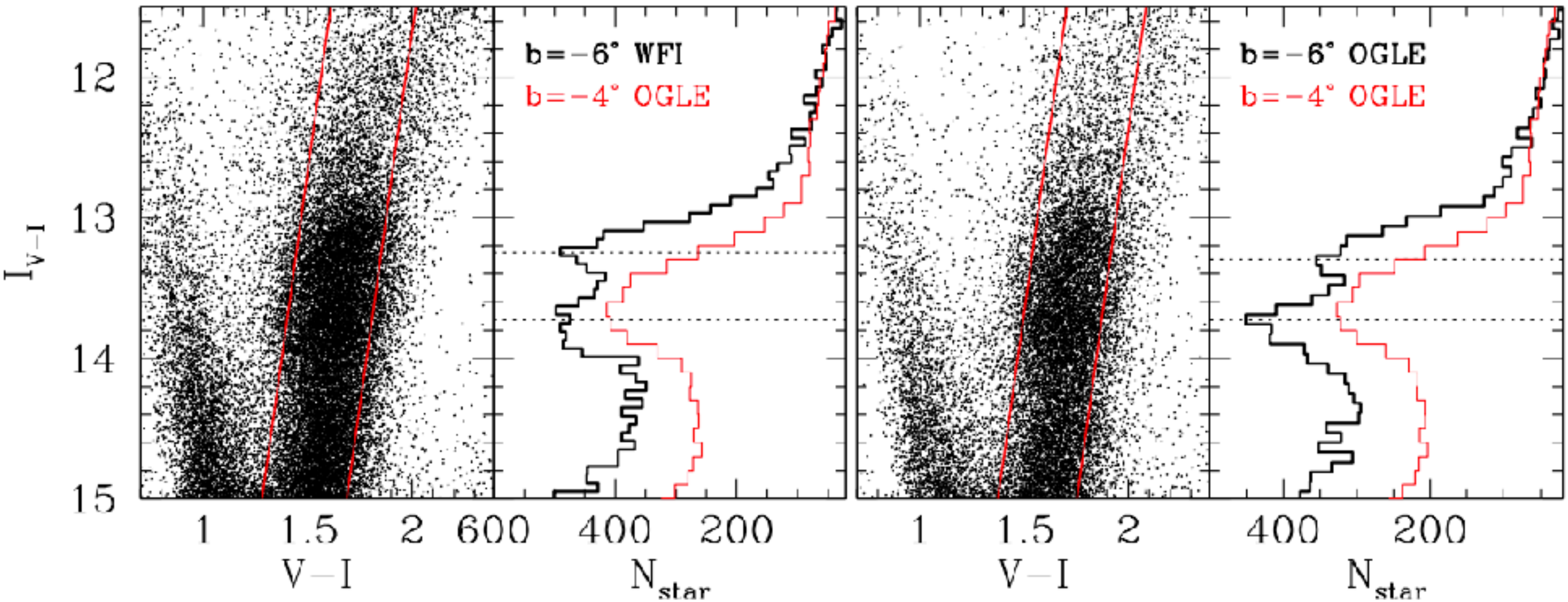

McWilliam and Zoccali (2010)

Double red clump

Clear at b=-6°, not clear at b=-4°

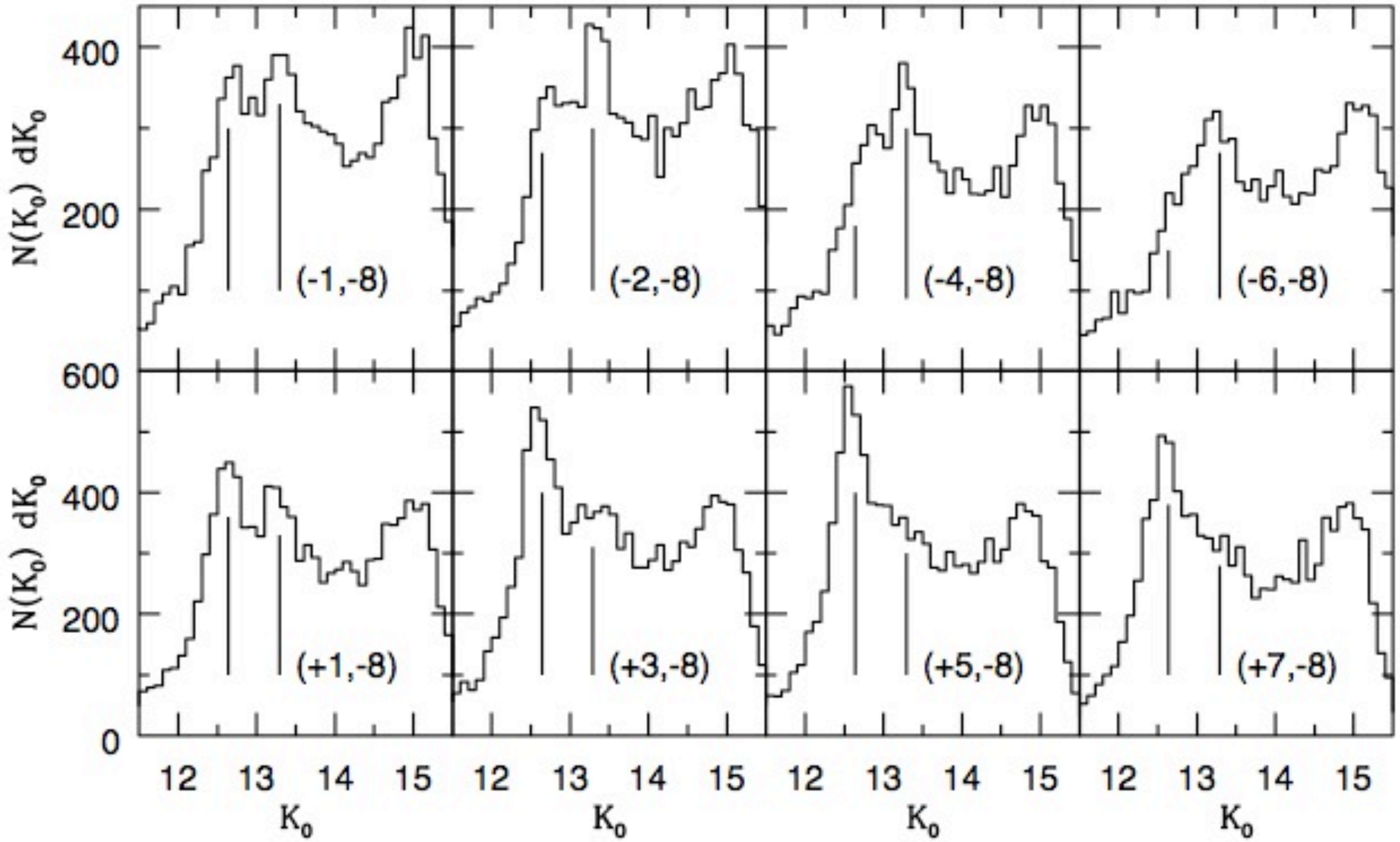

Double clump in different directions
=> 2 peaks of density at different distances

Projected distances to red clumps at b=-8

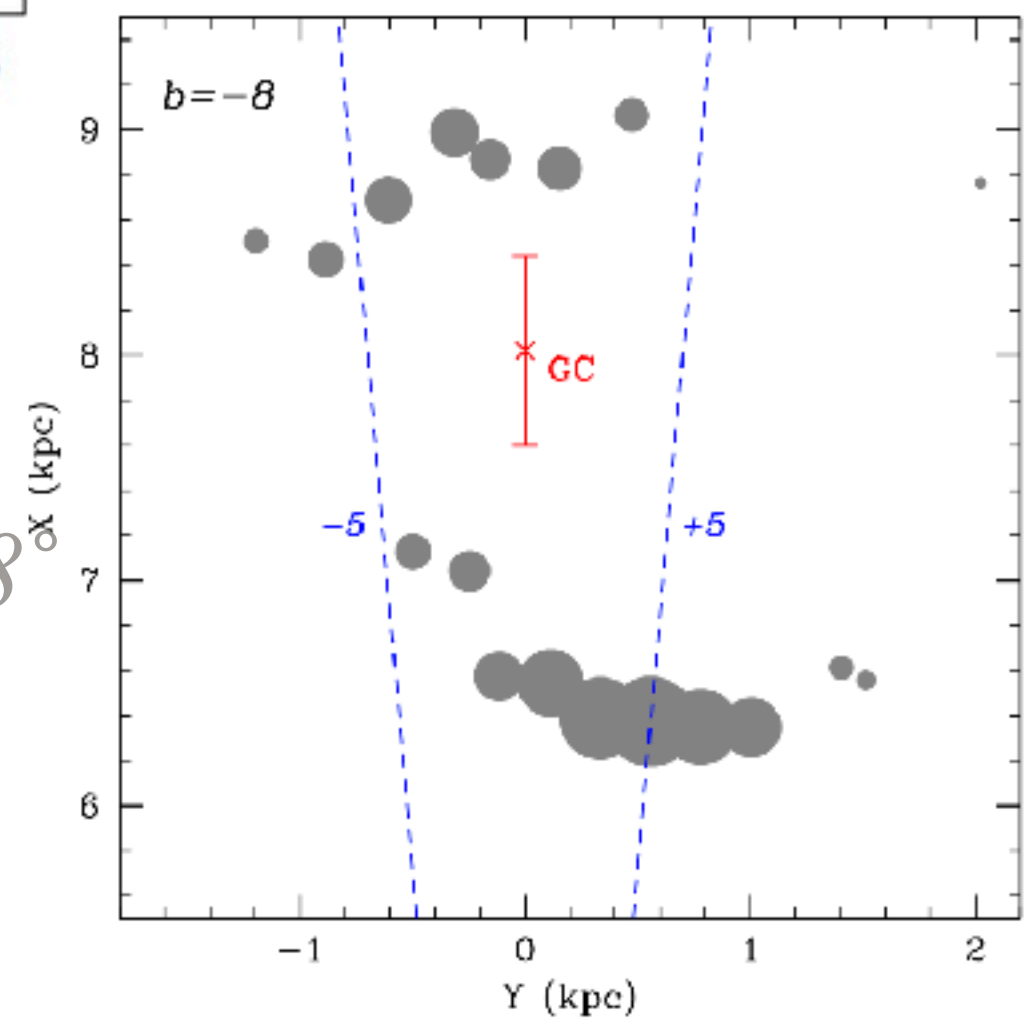

FIG. 6.— Plot of RC distances, in the $b = -8°$ plane, for lon-

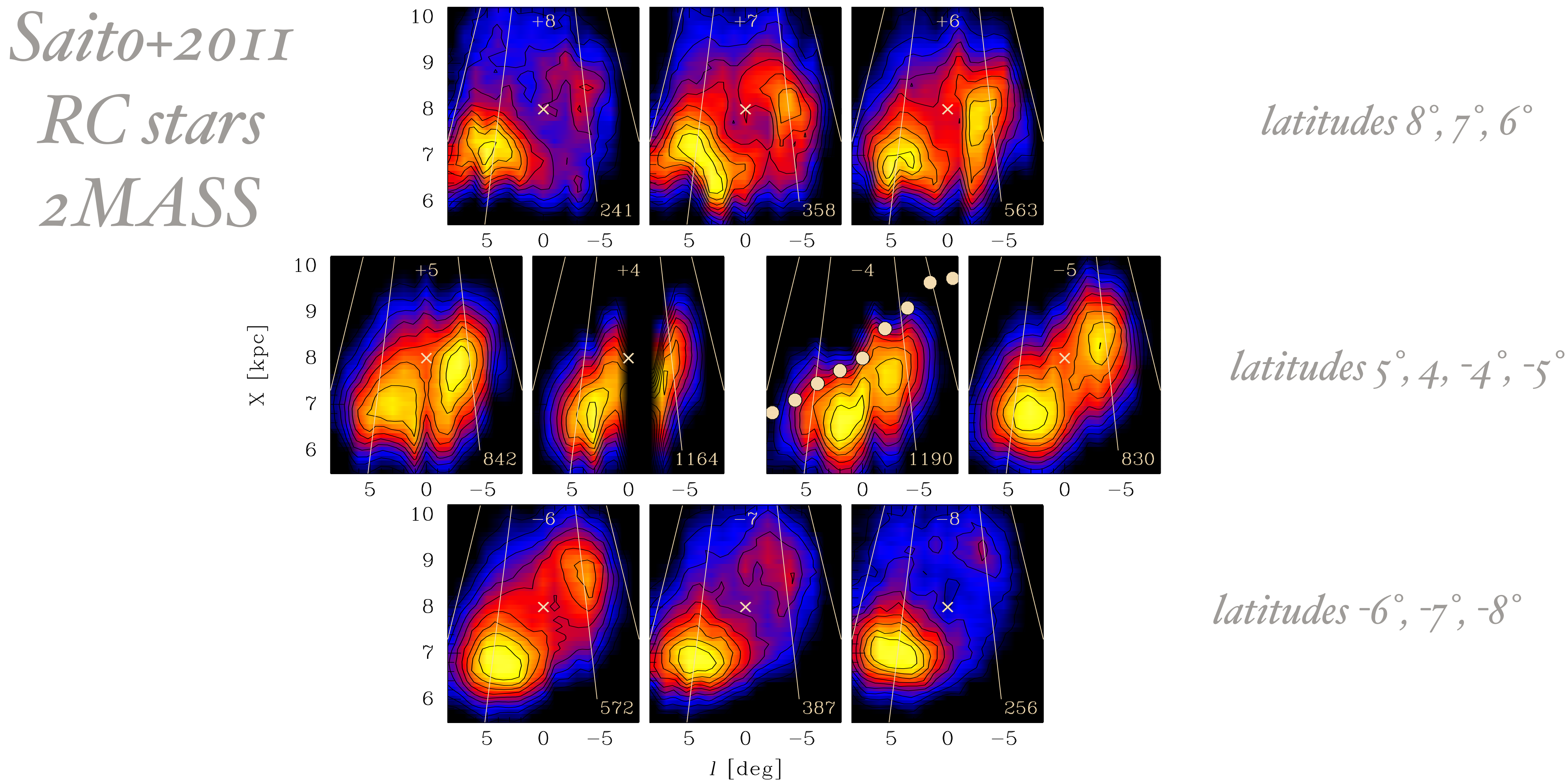

Fig. 3.— Density maps showing the structures traced by the RC near the Galactic plane, i.e., as seen from above, in slices of different latitudes (see labels). Individual lines of sight, at a given longitude, are represented by vertical strips, which are then merged together to form each panel. The central strip in each panel corresponds to $l = 0°$ with a cross marking the Galactic Center (assuming $R_0 = 8$ kpc). The panel at $b = -4°$ also shows the Galactic bar as traced by Rattenbury et al. (2007; white dots) fitting the RC in OGLE II data. The label at the bottom of each panel lists the peak value of the density histogram in that particular section of the 3D map. Contour plots may help the eye in regions of low density contrast. Thin white lines are lines of constant Y coordinate.

trace the shape of the bulge even far away from the plane, where stellar densities are much lower, but might give the wrong impression that the to-

longitudes, and the faint one at negative longitudes. The two overdensities get closer to each other for sections closer to the Galactic plane, and

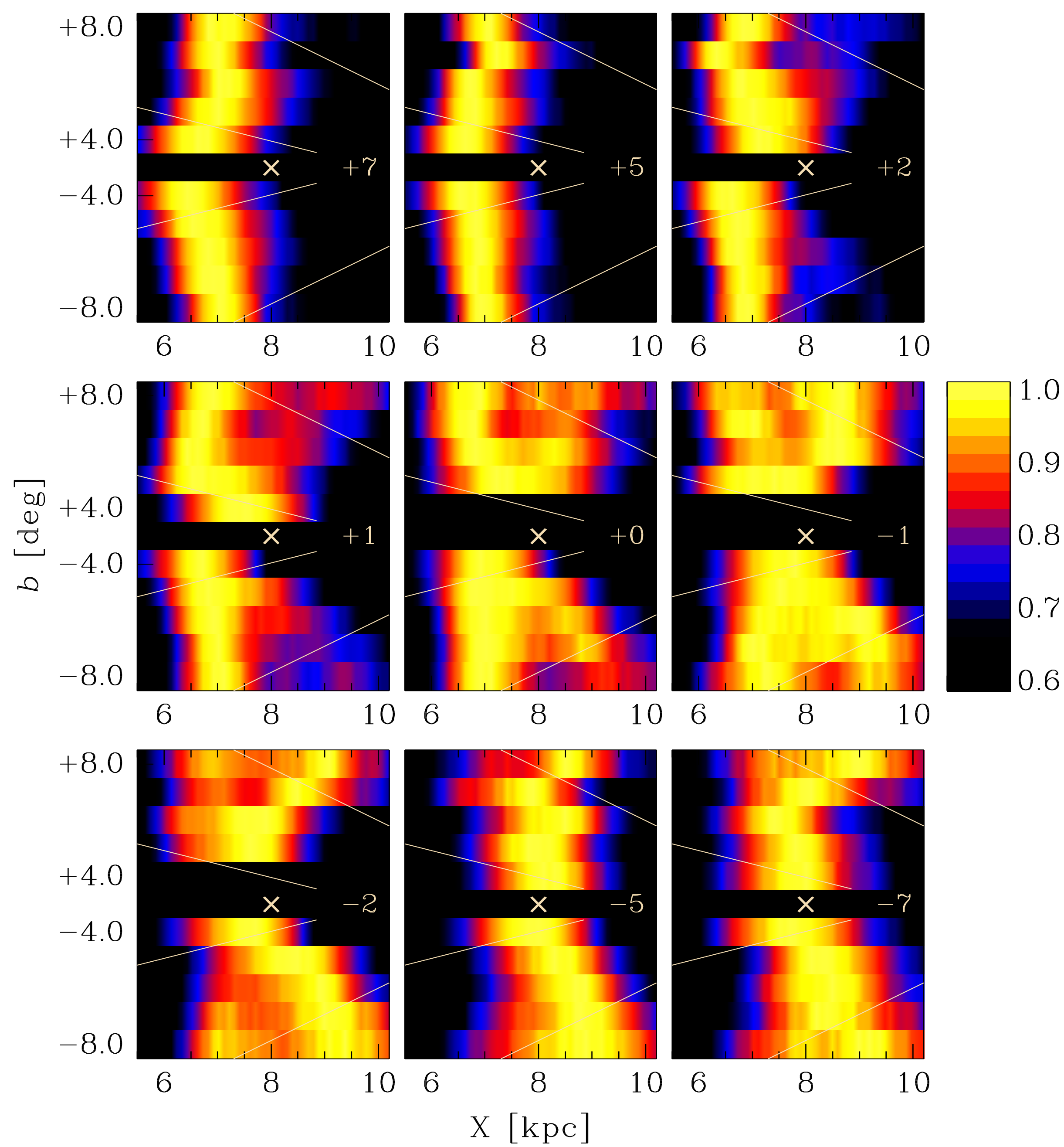

Fig. 4.— Density maps showing the structures traced by the RC in the (X, b) plane. Each panel corresponds to a different longitude (see labels), with $l = 0°$ in the central, middle one. A cross marks the Galactic Center (assuming $R_0 = 8$ kpc), with the Sun far in the left side, outside the figure, at $(X, Z) = (0, 0)$. Individual lines of sight, at different latitudes, correspond to horizontal color strips, merged together to form the panels. The color scale has been normalized so that the histogram peak in each horizontal strip has density=1. Note that the region close to the Galactic plane, for which we have no data, has been compressed here, and shown as a single, horizontal black strip. Thin white lines are lines of constant Z coordinate. The X-shape is clearly visible for longitudes $|l| \leq 1°$ (middle row panels).

- X-shape not seen at |b|<4°: no clear separation because the two arms are close and/or distances not accurate ?
- effect of extinction

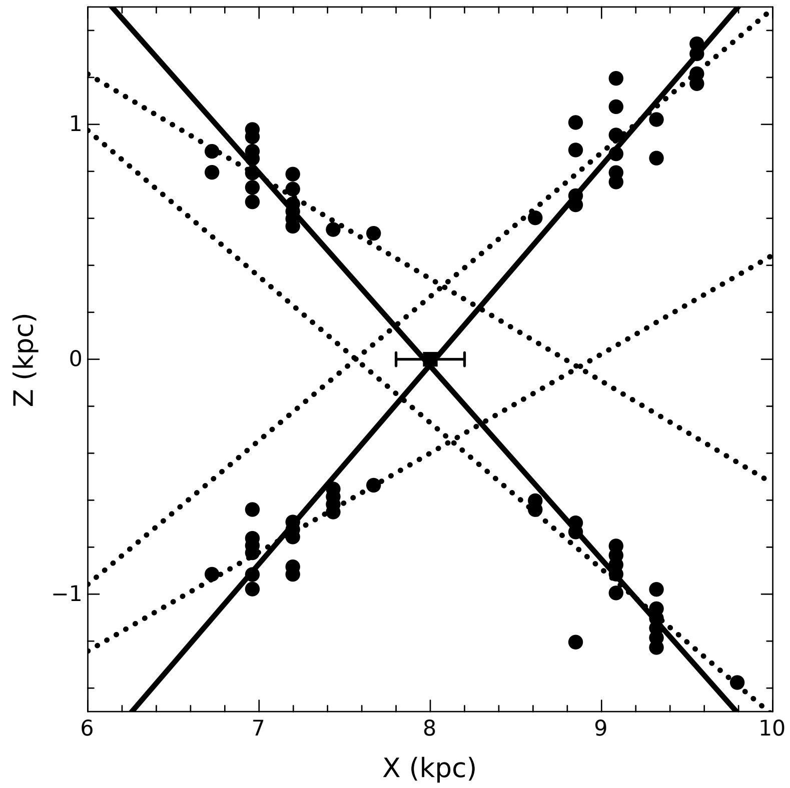

Gardner et al, 2013

X-shape or boxy shape ?

- Apparent X-shape (Ness & Lang, 2016 from WISE data): this is boxy !
- **X-shape from double-clump observations**
- Young F-dwarfs (< 5 Gyr): no X-shape (Lopez-Corredoira)
- Old (RR-Lyr, Miras) > 10 Gyr: No X-shape
- Clue for age of the bar buckling

X-shape bar ? a scenario

- Two main populations:
  - Thick disc with no X-shape (but influenced by the bar potential)
  - Bar with X-shape (ages ~5-10 Gyr)
  - Thin disc: formed after the bar, no clear X-shape

A scenario: Debattista et al, 2017:

- From a pre-existing disc, populations with low velocity dispersion suffer more the bar instability=> bar kinematics and X-shape due to bar orbits
- populations with high velocity dispersion (« hotter ») suffer less and show only a boxy peanut without X-shape

Clues for this scenario

- X-shaped structure in B/PS bulges is formed of relatively metal-rich stars that have been vertically redistributed by the bar, whereas the metal-poor stars have a more uniform, box-shaped distribution. *Gonzales et al. 2017, 2017MNRAS.466L..93G , from observations of external B/PS bulges.*

- Cylindrical rotation is generally considered one of the hallmarks of a bar-dominated boxy/peanut bulge, from N-body simulations of buckled bars, and from observations of external galaxies (Zasowski, Ness et al, 2017)

- Mean velocity of the Milky Way's inner regions is very weakly dependent on latitude (e.g., Howard et al. 2009; Zoccali et al. 2014, Paper I)

Kinematics and dynamics

- Dynamics is complexe, due to non-axisymmetries
- No simple analytical models
- N-body simulations : none ressembles the Milky Way exactly
- Use diverse N-body simulations (Debattista (2006), Shen et al (2010), Gardner et al (2013), Di Matteo et al (2016), Fragkoudi et al, (2017), among many others)
- M2M method to fit the N-body to observations (Portail & Gerhard, 2015)
- Other approaches: mass modeling from star counts + test particles (Fernandez-Trincado, PhD and in prep)
- Impact on microlensing: bar pattern speed effect on the Einstein radius crossing time distribution (see below)

Exemples of orbits

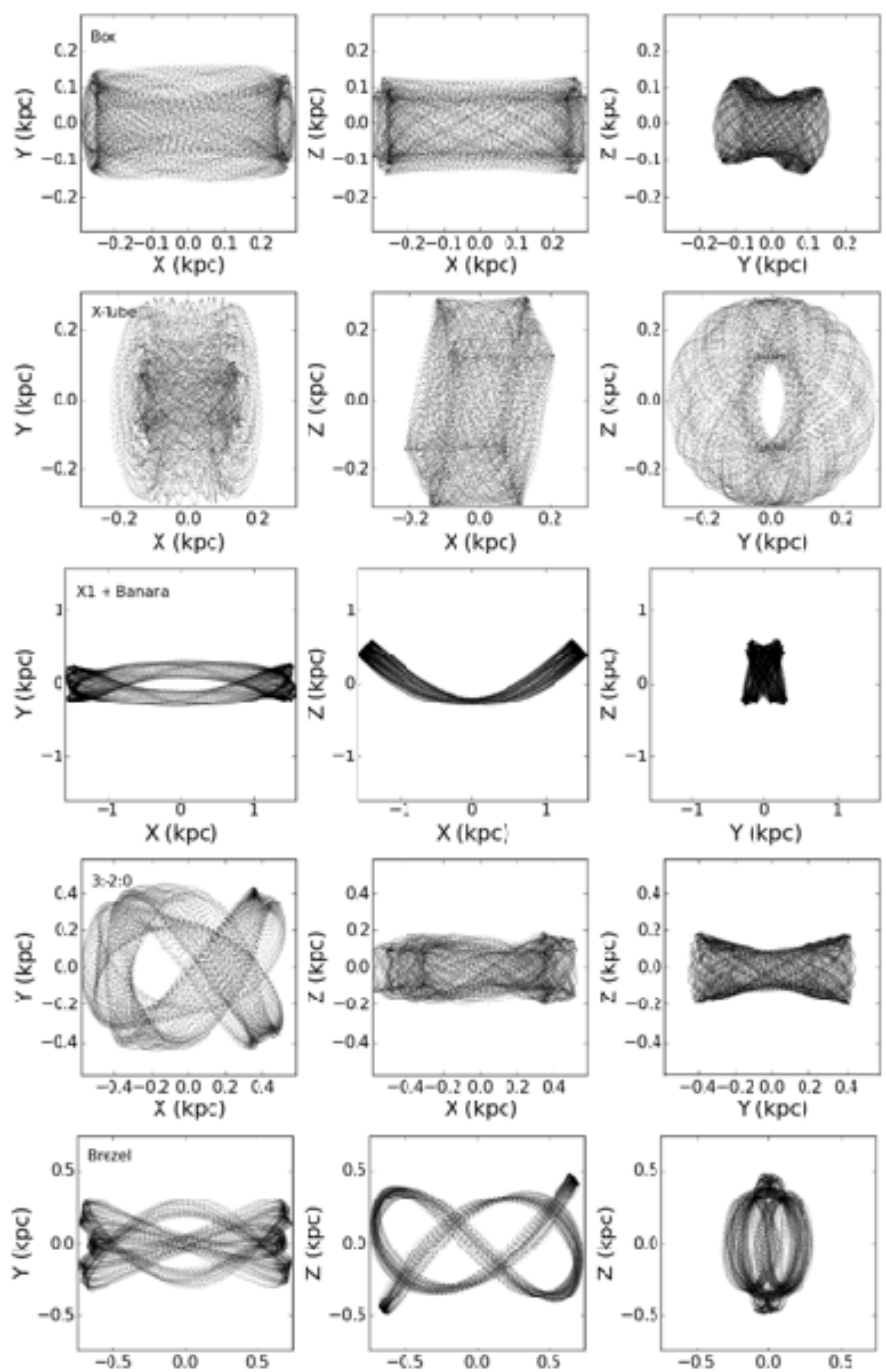

Abbott et al, 2017:

From the top to bottom: a box orbit, an x-tube orbit, an x1+banana orbit (2:-2:1), a fish/pretzel orbit (3:-2:0), and a brezel orbit (3:0:-5).

Bulge/bar density and mass

	Angle	xo	yo	zo
Vanhollebeke+2009	15° ±13.3 12.7	2.5 ±1.73 0.16	0.68±0.05 0.19:	0.31±0.06 0.04
Robin+2012	13° ±3.6	1.46±0.54	0.33	0.27
Wegg & Gerhard 2013, 2015	27° ±	0.70	0.63	0.26
Simion et al 2017	21°	1.78	0.44	0.29

Dynamical mass: Portail et al, 2015, 2017: 1.2-1.6 $\times 10^{10}$ M_{sun}

From light : Robin et al (2012): 0.67$\times 10^{10}$ M_{Sun} (for bar only)

Simion et al (2017): 2.36 $\times 10^{10}$ M_{Sun}

From Red clump stars: Valenti et al (2016): 1.7-2.3 $\times 10^{10}$ M_{Sun} (but selecting all population within $-9.5° < l < 10.5°$ and $|b| < 4.5°$)

Constraints from spectroscopy

- Kinematics, metallicities, abundances => clues for understanding the bulge populations.
- However, spectroscopic surveys are incomplete. Selection bias to be corrected.
- Kinematics vs metallicity: chemodynamical evolution
- Main surveys :
    - BRAVA: Rich et al, 2011, Kunder+2012 2012AJ....143...57K
    - GIBS: Zoccali+2014, Zoccali+2017 2017A&A...599A..12Z
    - ARGOS: Freeman+2013 2013MNRAS.428.3660F, Ness+2013 013MNRAS.430..836N, 2013MNRAS.432.2092N
    - APOGEE: Zasowski+2016 2016ApJ...832..132Z,Ness+2106 2016ApJ...819....2N, Garcia-Perez+2013 2013ApJ...767L...9G, Schultheis+2017 2017A&A...600A..14S

ARGOS survey

Ness et al (2013)

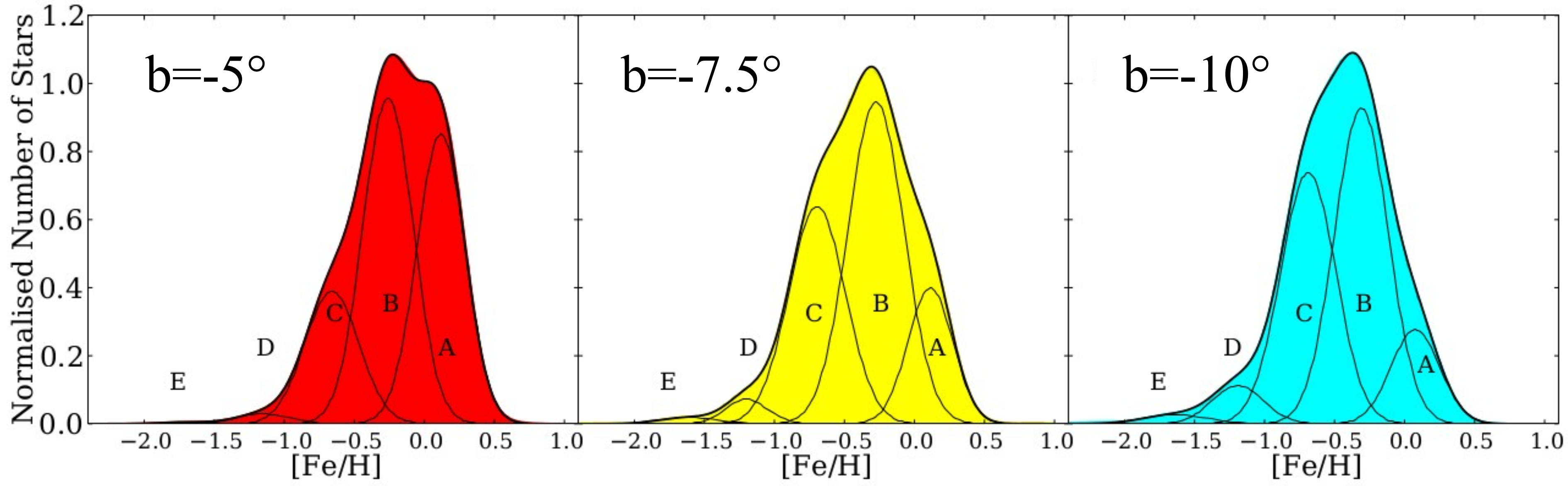

- Several populations (A to E) which contribute differently at different latitudes (different scale heights)
- Decomposition varies from authors to authors
- Agreed on : barred thin disc, thick disc, inner halo
- May be a classical bulge (small < 8% from Shen et al 2010)

Gaia-ESO survey

l ~-6° *l ~0°* *l ~+7°*

b~-4°
b~-6°
b~-8°
b~-10°

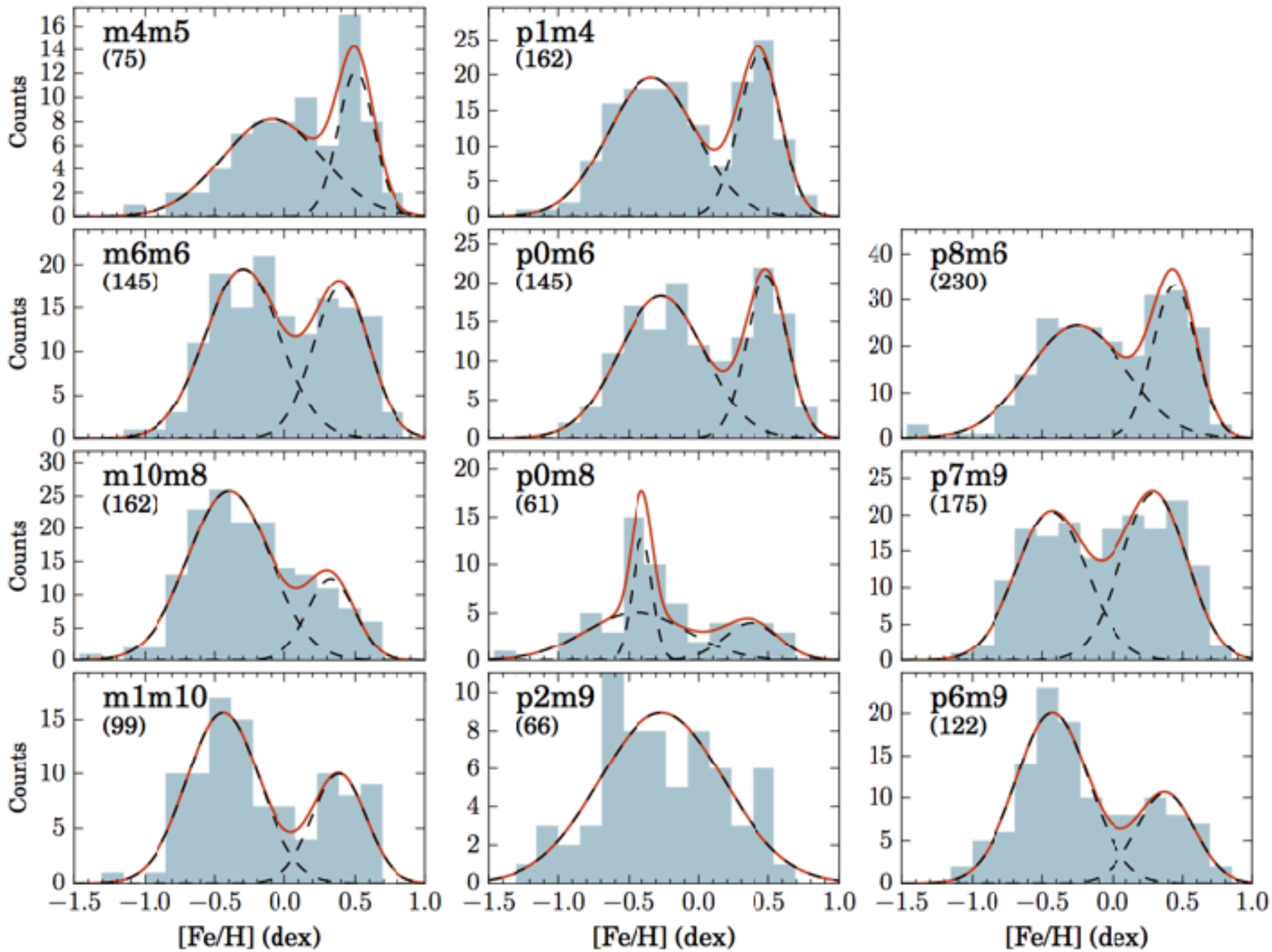

Rojas-Arriagata et al (2017)

Gaia-ESO survey

Babusiaux et al

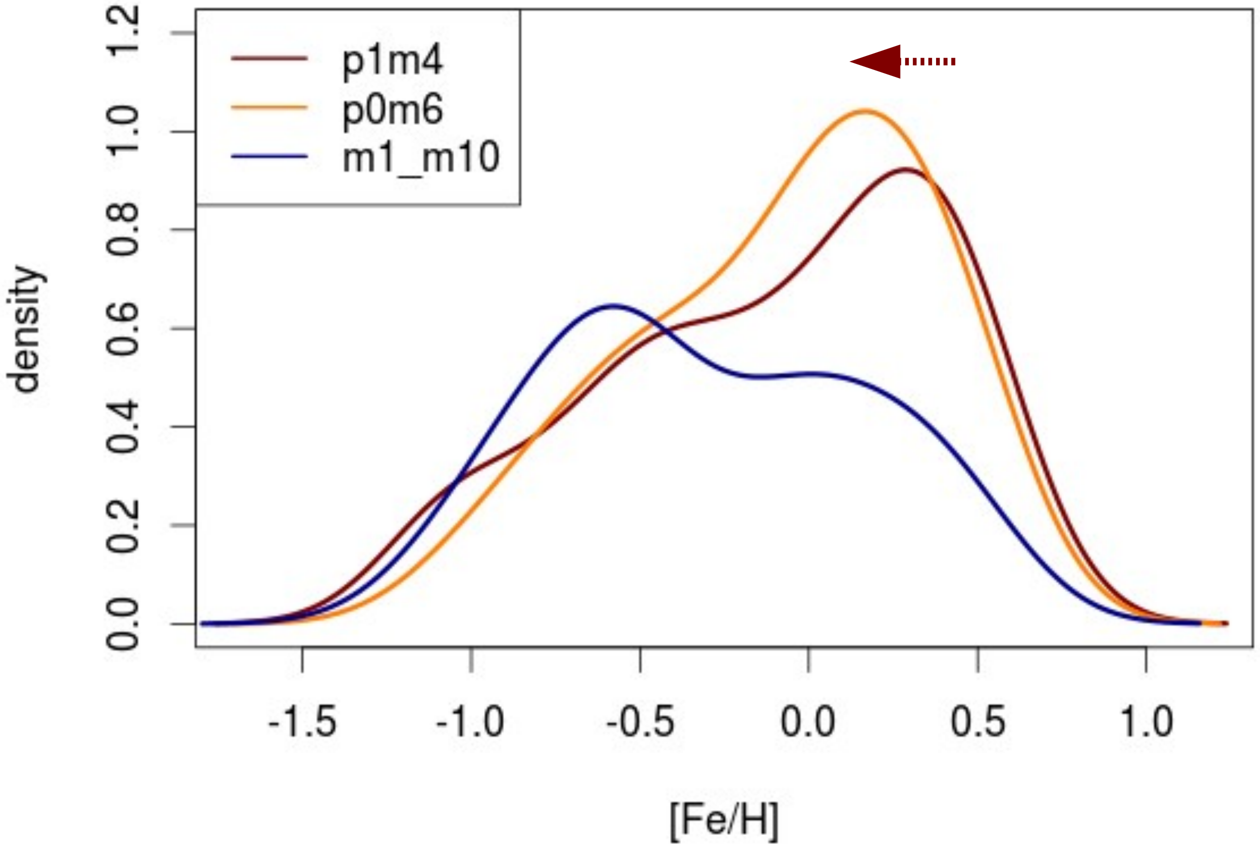

- The proportion of population changes with latitude=> mimic a metallicity gradient
- Thick disc contribution important at |b|>=8°

Chemo-dynamics

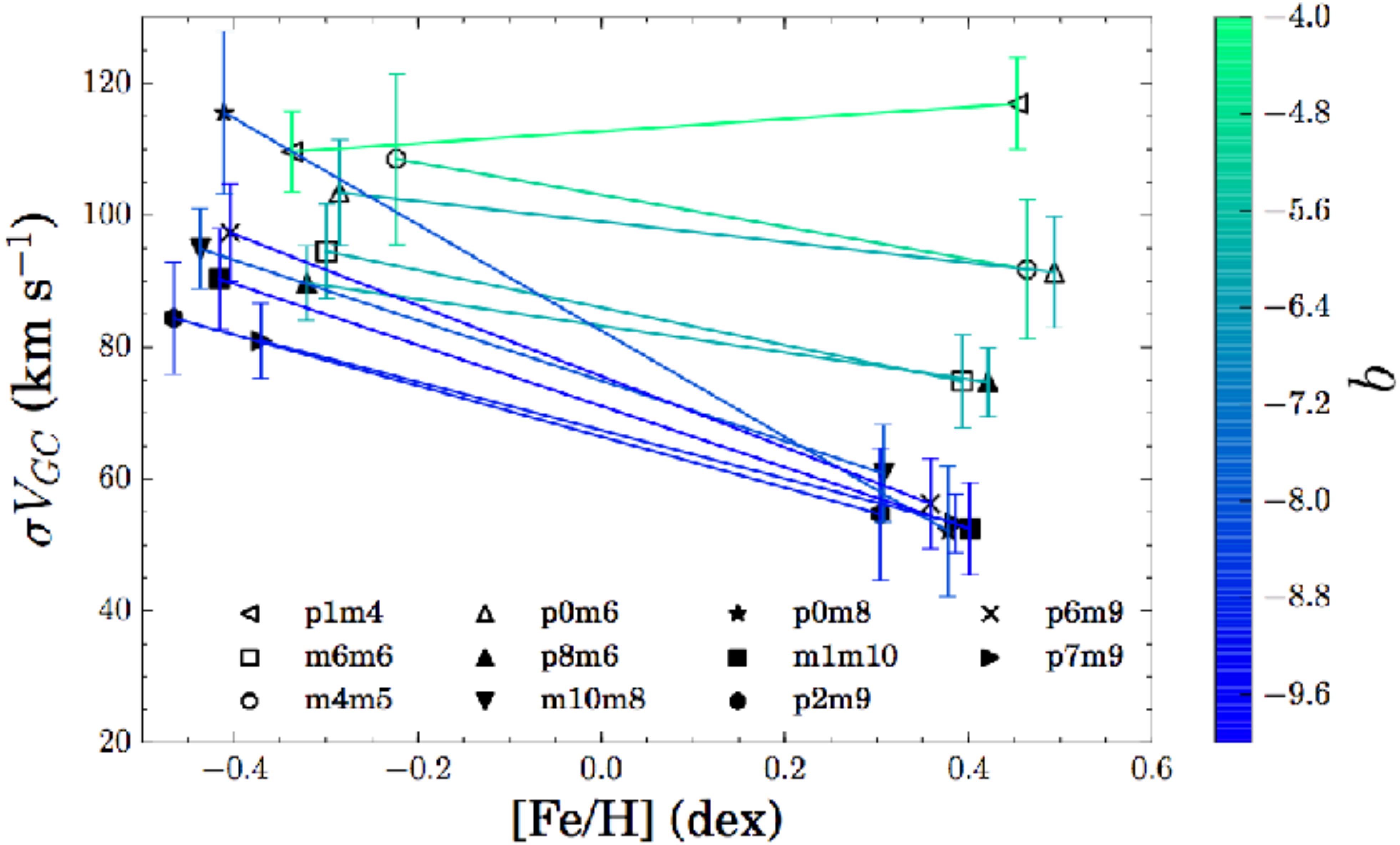

Rojas-Arriagata et al (2017)

- The metal rich population has a vertical velocity dispersion gradient
- Not the metal poor population (thick disc)

The Besançon galaxy model:

a population synthesis approach

Population synthesis aims

- Seeing what amount of available **survey** data !
- Diversity of data (photometry, spectroscopy, astrometry, astero-seismology…)
- Diversity of tracers (many stellar types, ISM, even magnetic fields, cosmic rays…)

Can we imagine a global scheme for the Galaxy, its structure and its evolution ?

Synthesis : scenario & hypothesis => simulations

Physical processes : Stellar physics, Galactic dynamics, ISM light transfer…

Population synthesis

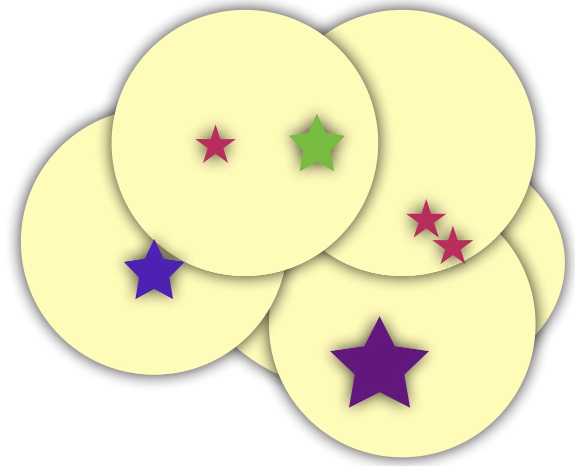

Start with a mass of gas
=> Transform into stars as functions of IMF and SF History

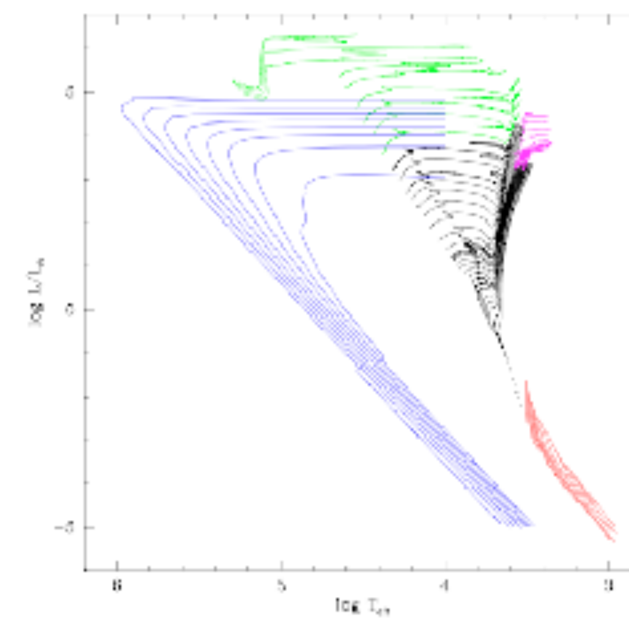

Stars evolve on evolutionary tracks
and populate the HR diagram

Proceed for each population according to its SFH
=> ***φ(Teff, log g, age)***

Important ingredients : SFH, IMF, stellar models, atmospheres

3D extinction map

φ(Teff, logg) for a thin disc decreasing SFR over 10 Gyr

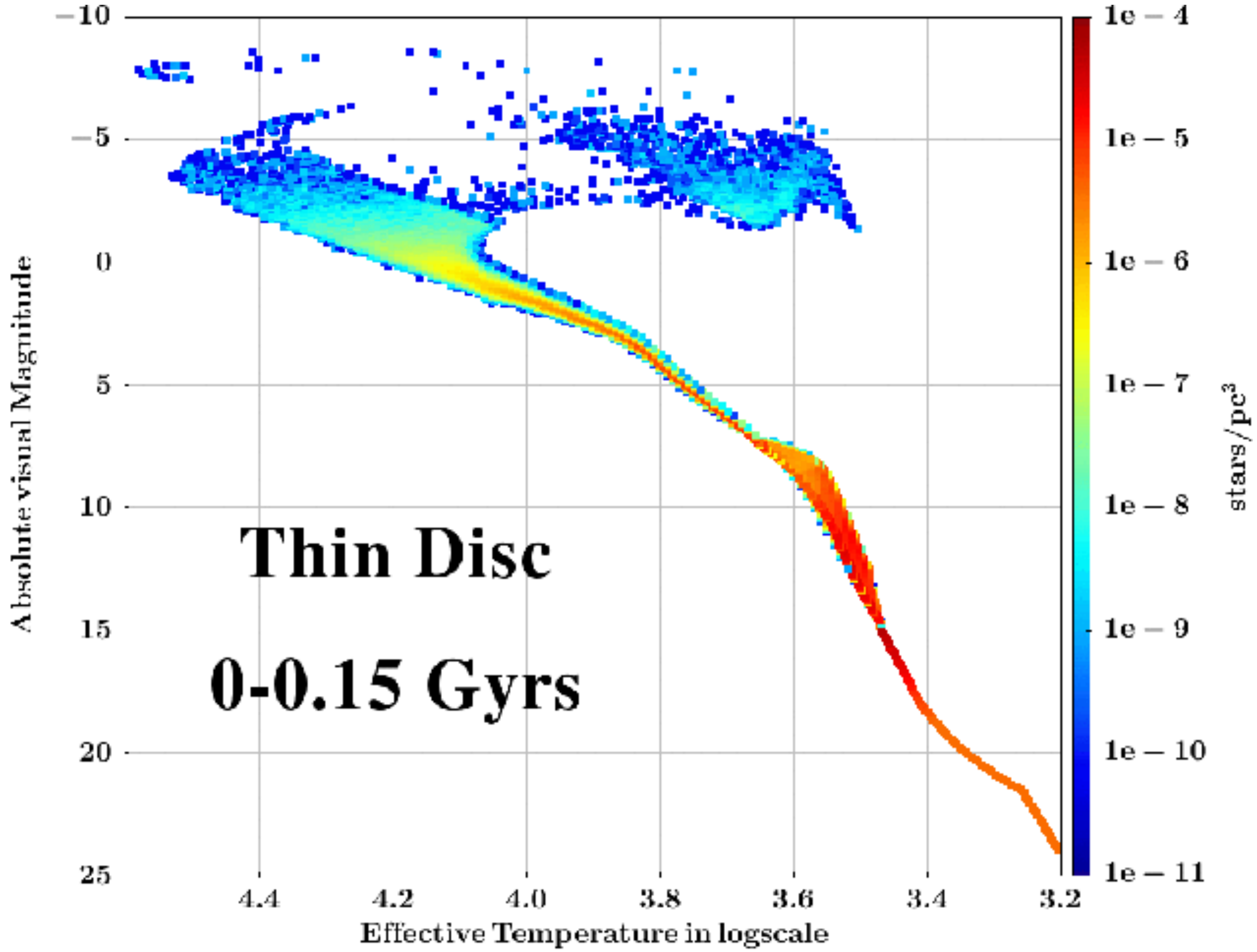

Mor et al, 2016

Population synthesis

Equation of stellar statistics

Simulation
of stars along a
line of sight

$$N = \int_0^{\infty} \rho(r)\, \phi(M)\, \Omega\, r^2\, dr$$

or

$$N = \sum_{i=1}^{Npop} \int_0^{\infty} \rho_i(r)\, \phi_i(M)\, \Omega\, r^2\, dr$$

ρ(x,y,z) : density laws
constrained by dynamics
(Bienaymé et al, 1987)

ϕ(*Teff, log g, age*)

3D extinction model

Simulate
observational errors
and selection function

Bulge populations as of BGM

- Thin disc : mainly foreground: 1 to 10 Gyr, metal rich, differential rotation
- Bar, 5-10 Gyr, metal rich, rotating as a solid body, pattern speed 35-60 km/s/kpc (or alternatively a N-body simulation from Fux (1999) or Debattista (2006))
- Thick disc, 9-12 Gyr, slightly metal poor, differential rotation but slowlier
- Halo, 12-13 Gyr, metal poor, radial motions, no rotation
- Maybe a classical bulge, 12-13 Gyr, radial motions, no rotation

Predicted metallicity distributions

APOGEE DR12

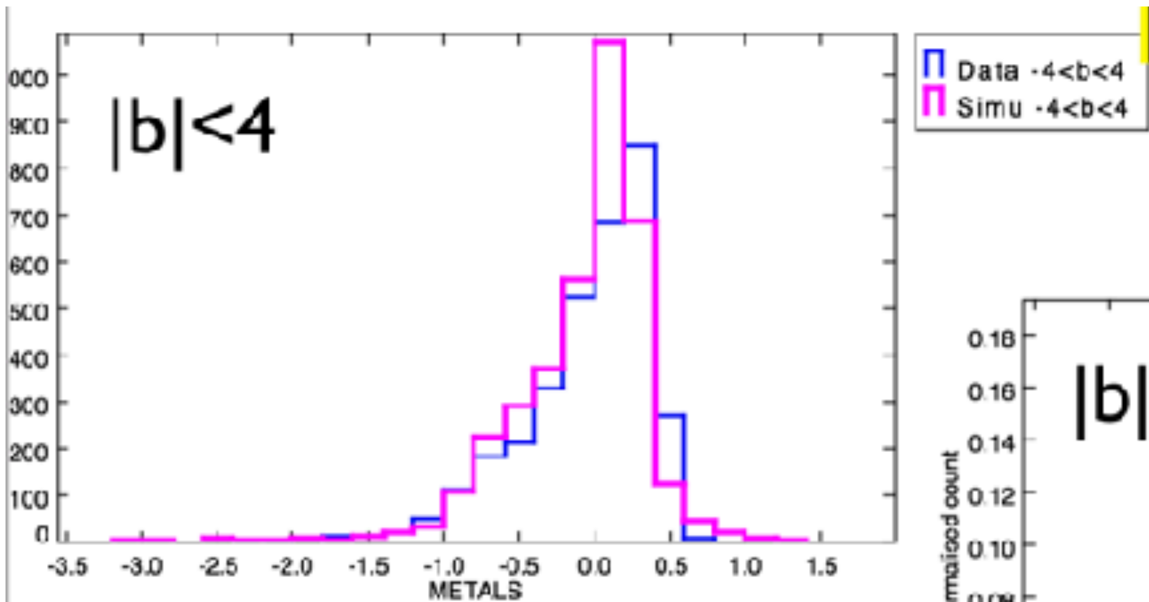

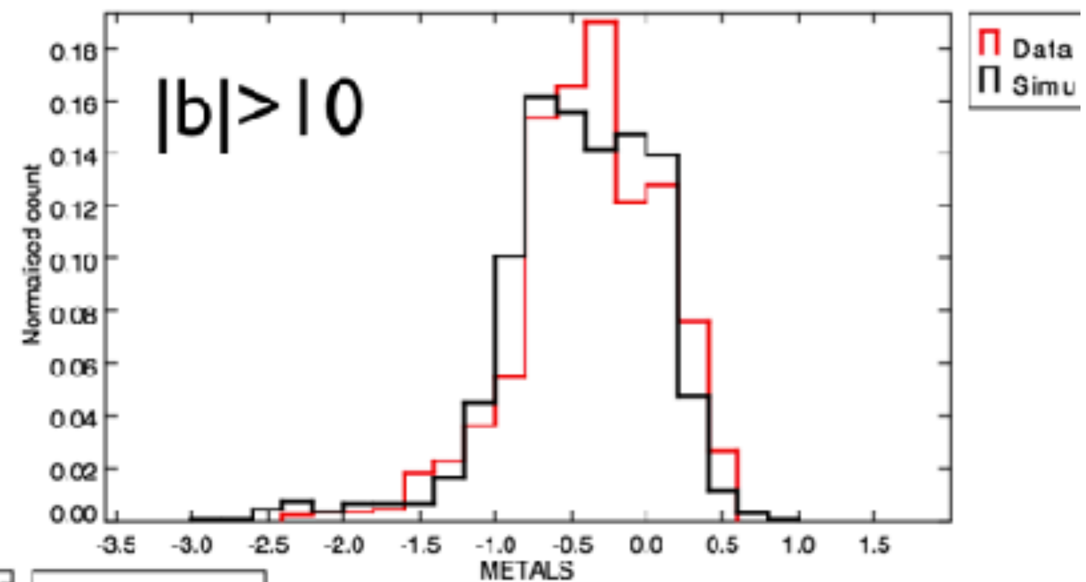

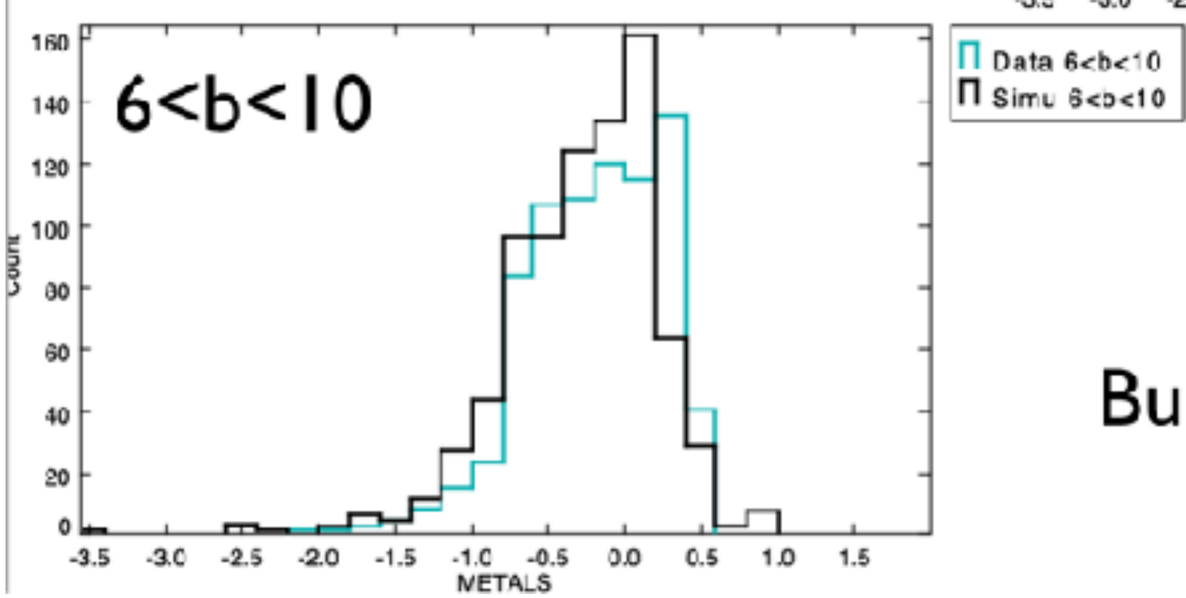

Bulge region -5°<l<18°

No fit

Other models

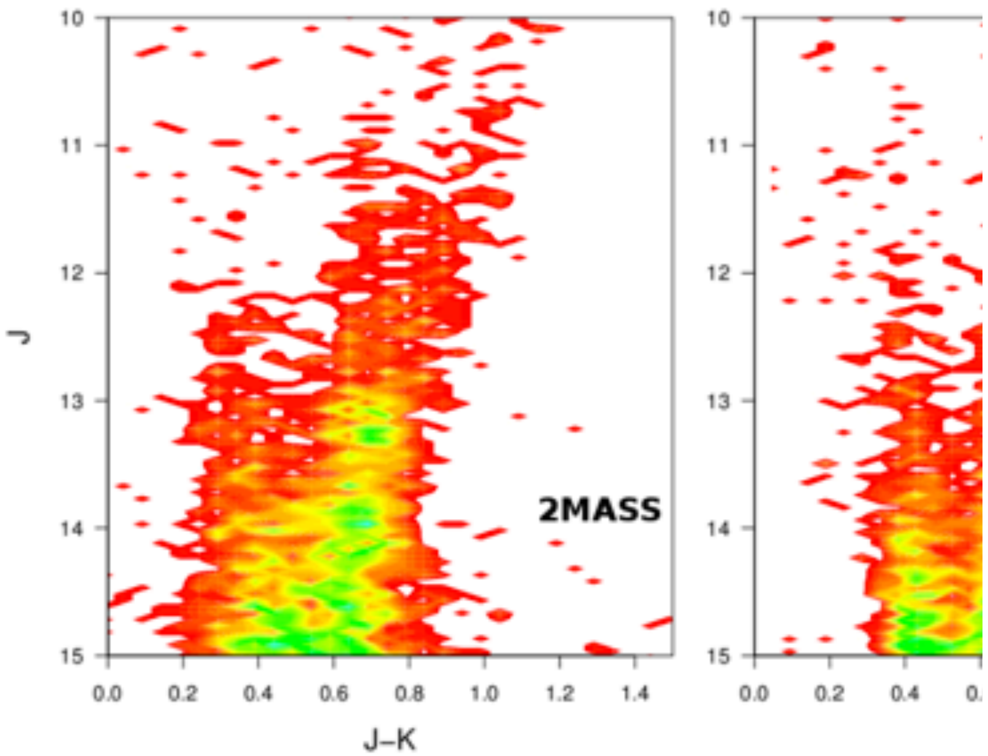

Fig. 21. Observed and simulated CMDs plotted as density maps. the Besançon model. *Right panel:* simulated CMD from the TRI density of stars are connected in the diagrams.

Uttenhaler et al, 2012

2012A&A...546A..57U

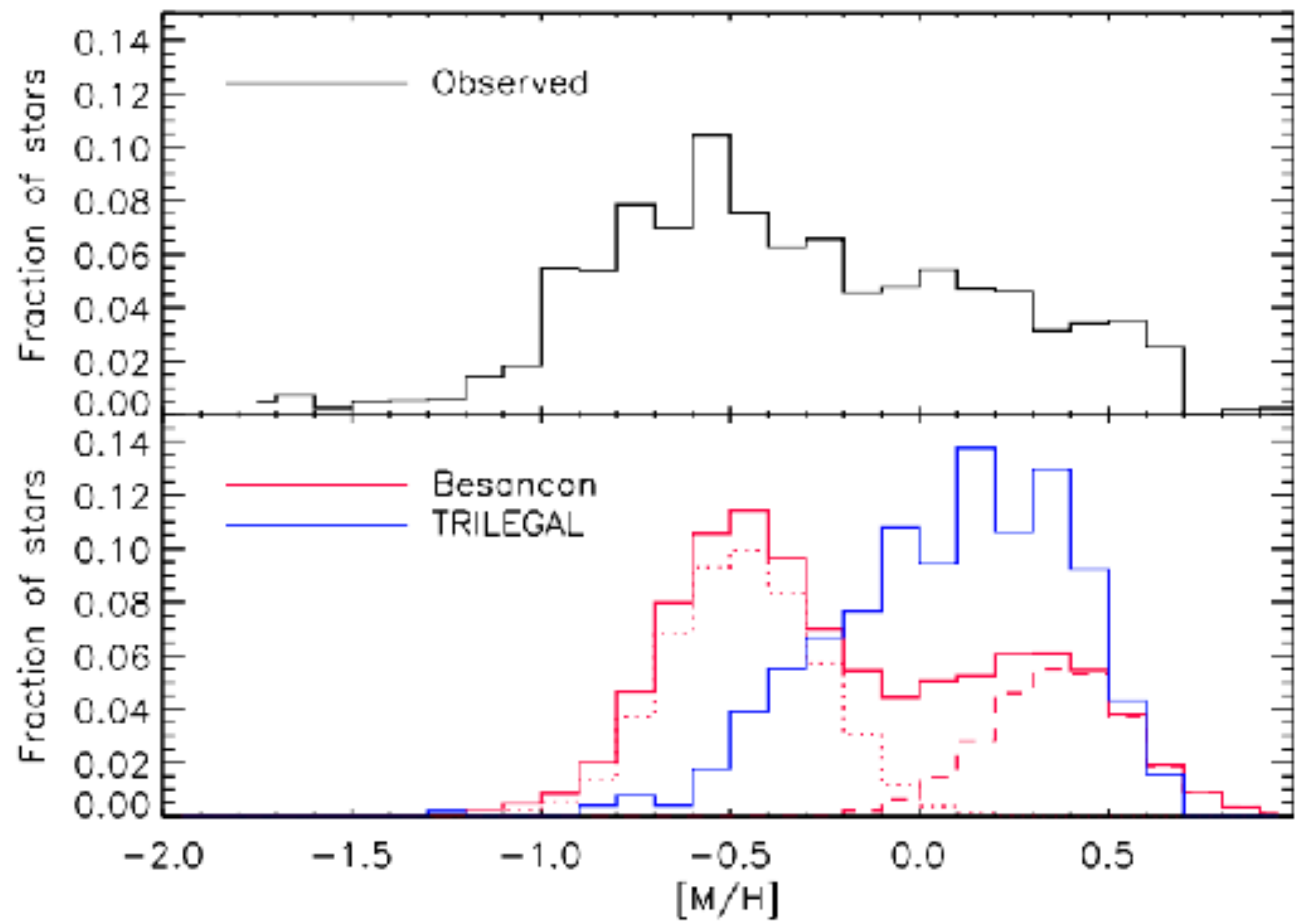

Fig. 12. Comparison of the observed MDF corrected for sampling effects (***upper panel***), with the ones predicted by the Besançon and TRILEGAL models in the selection region (***lower panel***). The histograms are normalised to the same area. In the lower panel, the red dotted line shows the MDF of "thick bulge" stars in the Besançon model, whereas the dashed red line is the one for the bar component.

Kinematics at the Solar neighborhood

- Simulating the RAVE survey selection function, radial velocities
- Gaia TGAS : accurate proper motions for the RAVE stars
- Separate stars by metallicity (4 bins) and by temperature (cool/hot)
- $|b|>25°$ to avoid extinction problems (and complex selection function)
- Fit kinematic model for the thin and thick disc (ABC-MCMC)

Robin, Bienaymé, Reylé, Fernandez-Trincado, 2017

- Solar motion
- Thin disc velocity dispersion as a fct of age
- Correct computation of the asymmetric drift out of the plane (Bienaymé +2015)

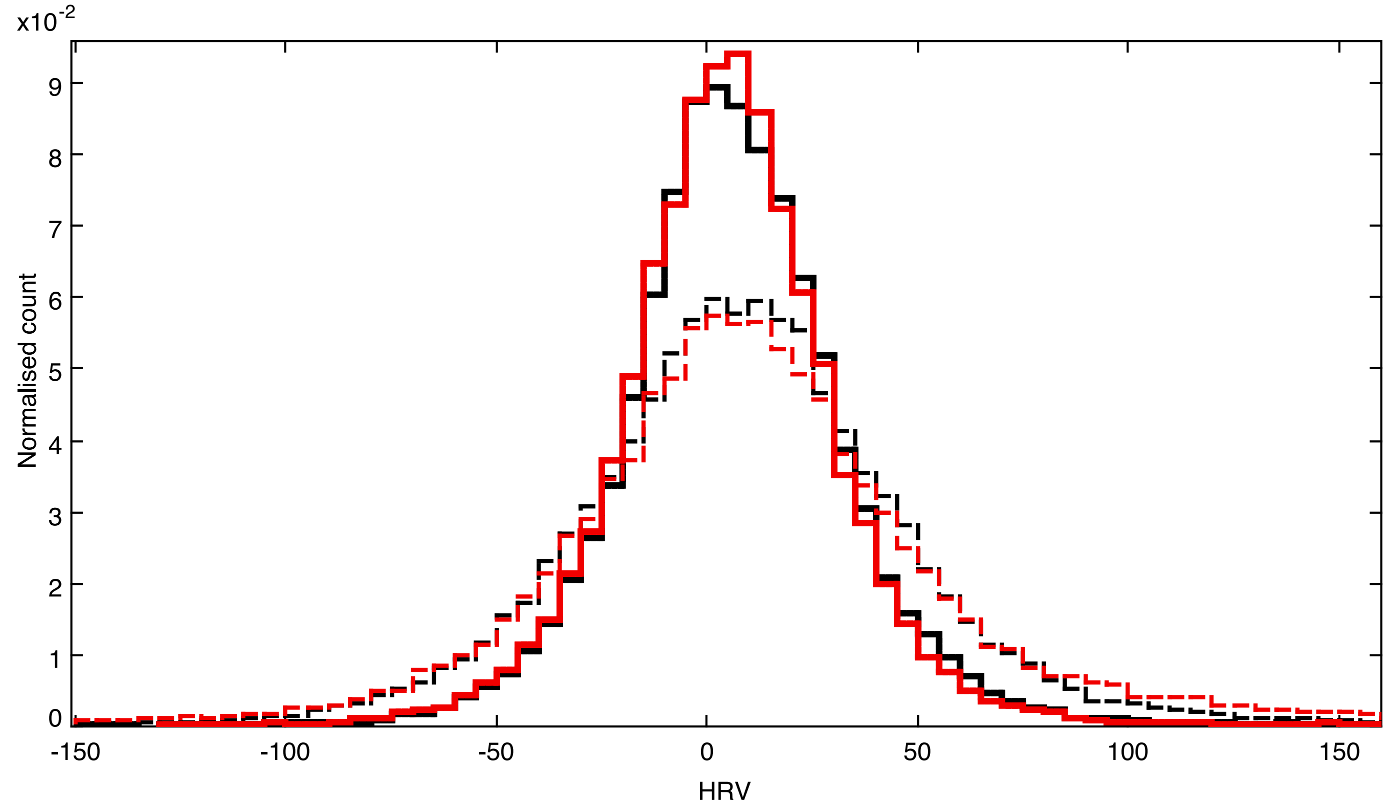

V_{los}

Hot: solid
cool: dashed

Data
Model

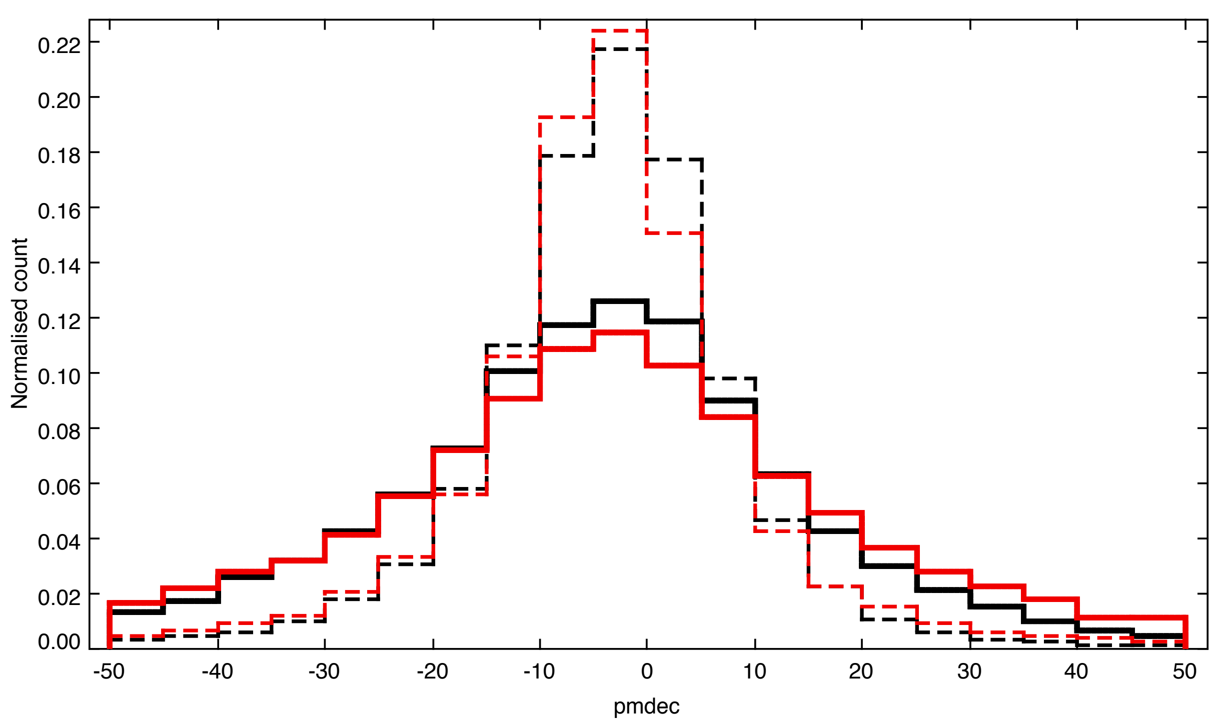

pm_{ra}

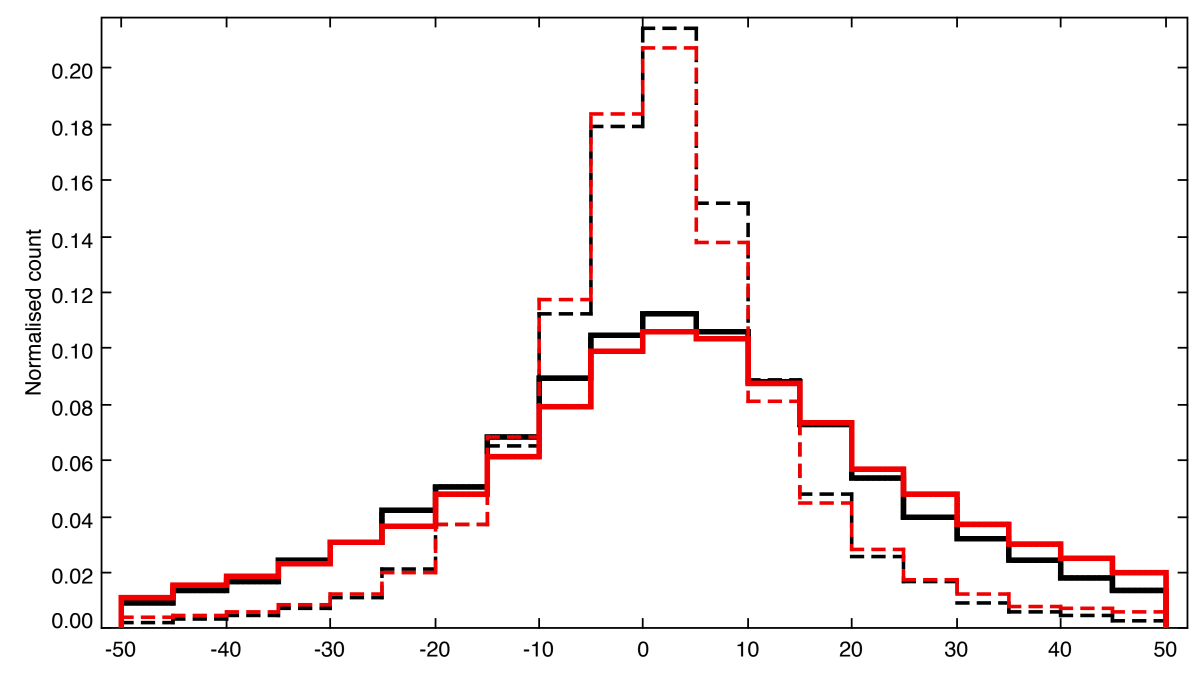

pm_{dec}

Predicted radial velocities in the bulge

- From N-body simulation dynamics (Debattista 2006) injected into Besançon model

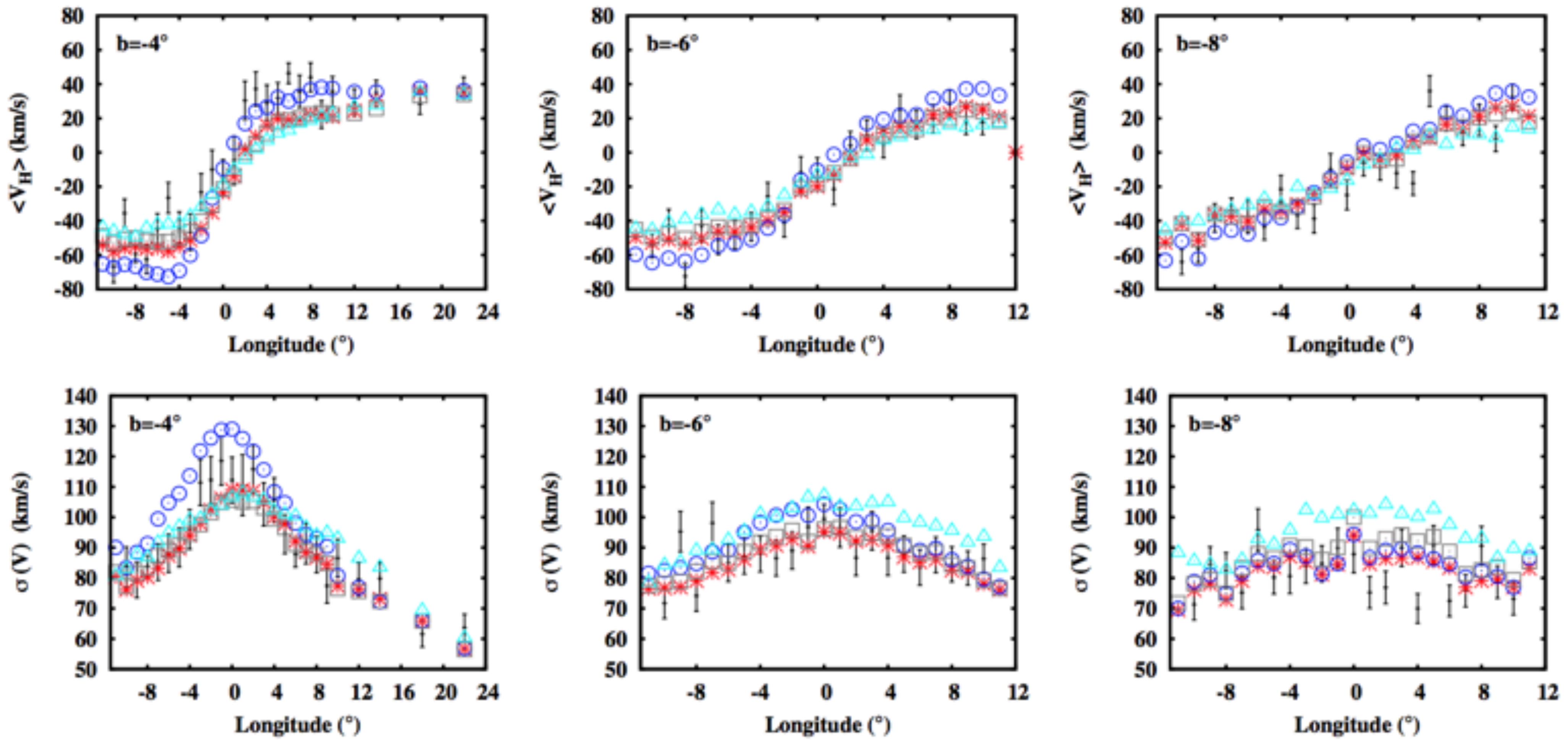

Figure 5. Mean heliocentric velocities and velocity dispersions for BRAVA fields along strips of $b = -4°$, $-6°$ and $-8°$. Data: point with error bars; Models : R1: grey squares, B3: red stars, R5: cyan triangles, Fux: blue circles. The model data have been obtained usin the BGM sampling velocities from the N-body models.

Microlensing predictions

- Kerins et al 2009: first estimates at different wavelength
- Awiphan et al (2016) extended simulations with revised population synthesis model
- Ban et al 2017: estimation of FFP at different wave length and field of view
- http://mabuls.net : simulator of microlensing maps in the bulge
- Problems with missing mass to reproduce MOA ?

Comparison of BGM-2012 microlensing predictions with MOA-II

Awiphan et al, 2016, MNRAS 456,1666

- Simulations of MOA-II fields (Sumi et al. 2011, 2013)
- average time scale and event rate toward the Galactic bulge are calculated using all combinations of source and lens pairs from source/lens catalogue simulations
- Compute all resolved sources above a specific magnitude threshold and also from all difference imaging analysis (DIA) sources which have a magnified peak above the same threshold
- Extend BGM to lower mass stars and brown dwarfs

Microlensing event rate per star

Resolved sources | *All sources*

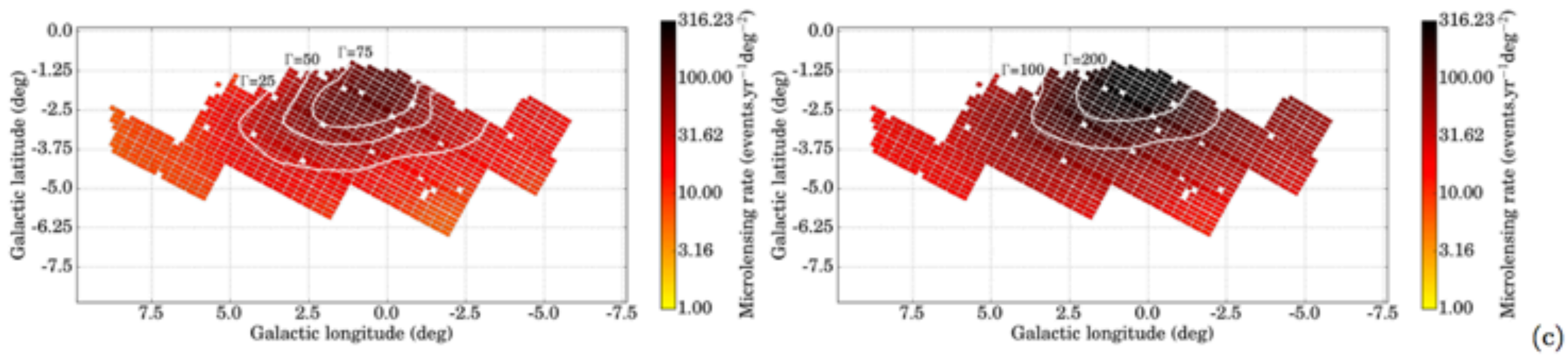

Microlensing event rate per square degree

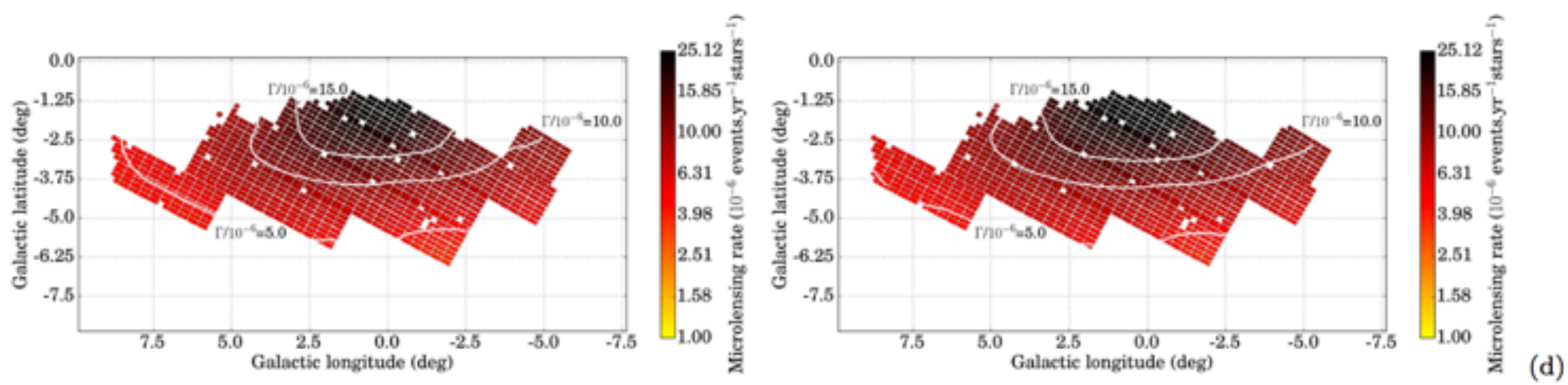

Microlensing event rate per star

Residuals MOA-II / BGM

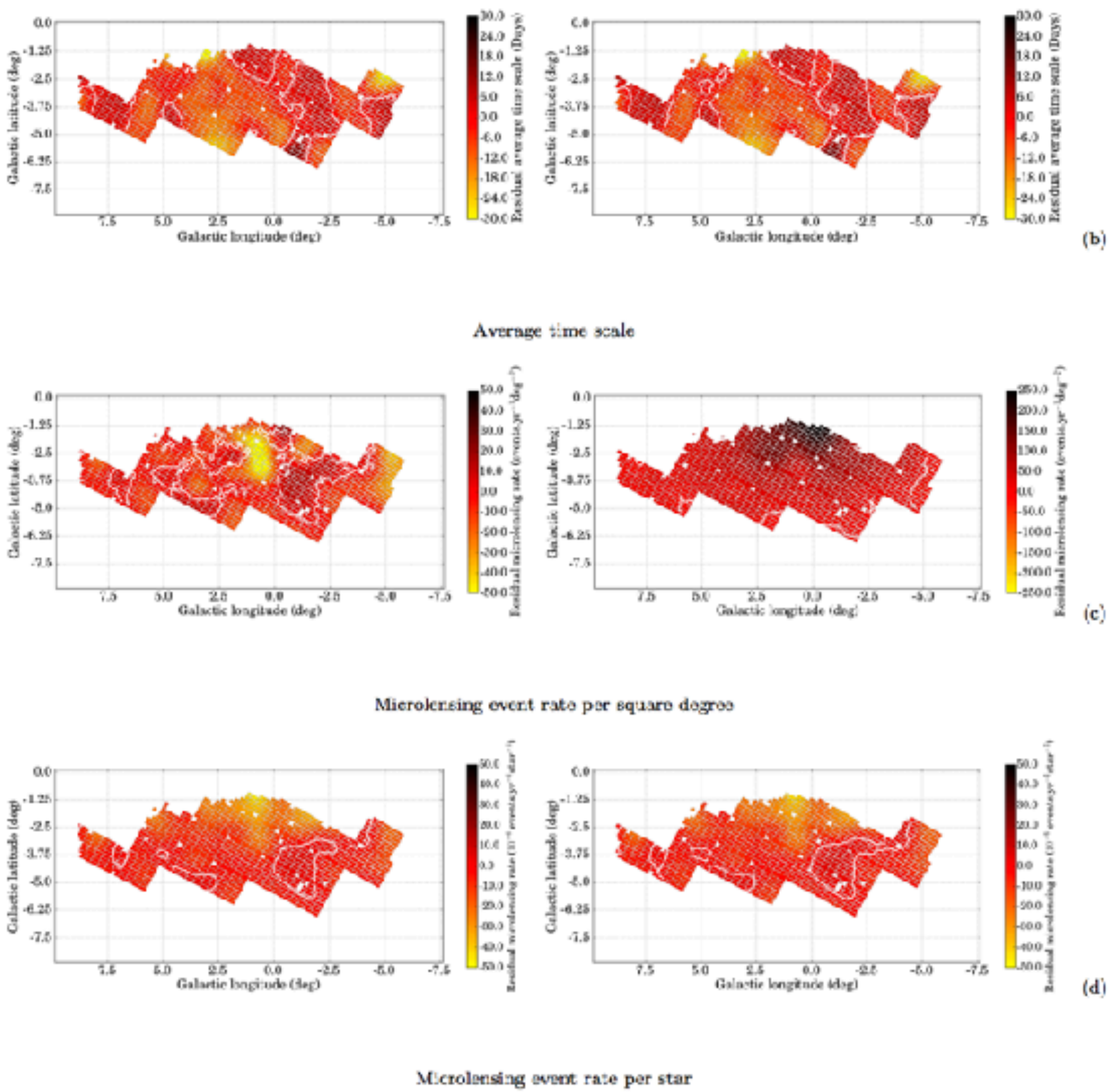

- Hot spot ! however to be revised with MOA-II corrected from incompleteness

Average time scale maps from BGM

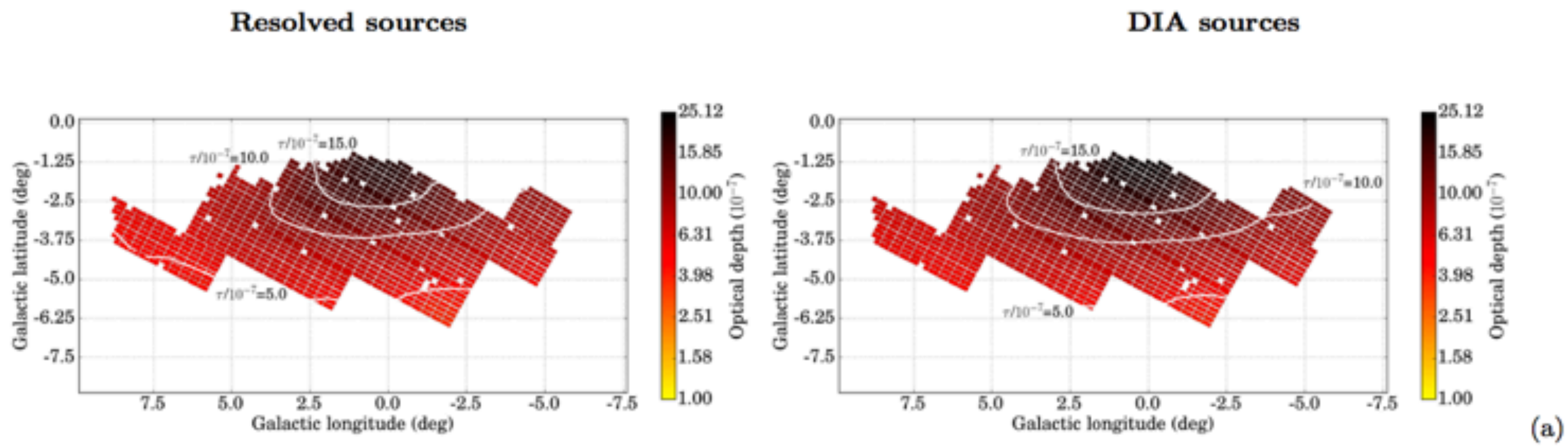

Optical depth

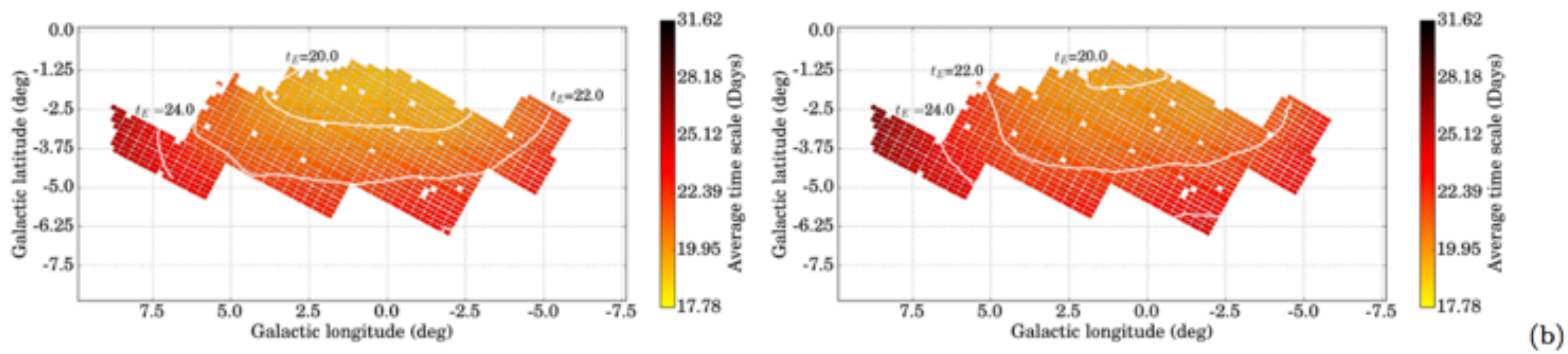

Average time scale

Event time scale

- The residuals of the distribution (model – data) with adding low-mass stars show a **slight deficit of events with short crossing time between 0.3 and 2 days and very long crossing time between 30 and 200 days.** Moreover, the model tends to over-predict the number of events with duration between 2 and 30 days, though there is **not a high statistical significance to any of these discrepancies (2.2 sigmas)**. Bulge model responsible from the discrepancy (kinematics or spatial distribution).

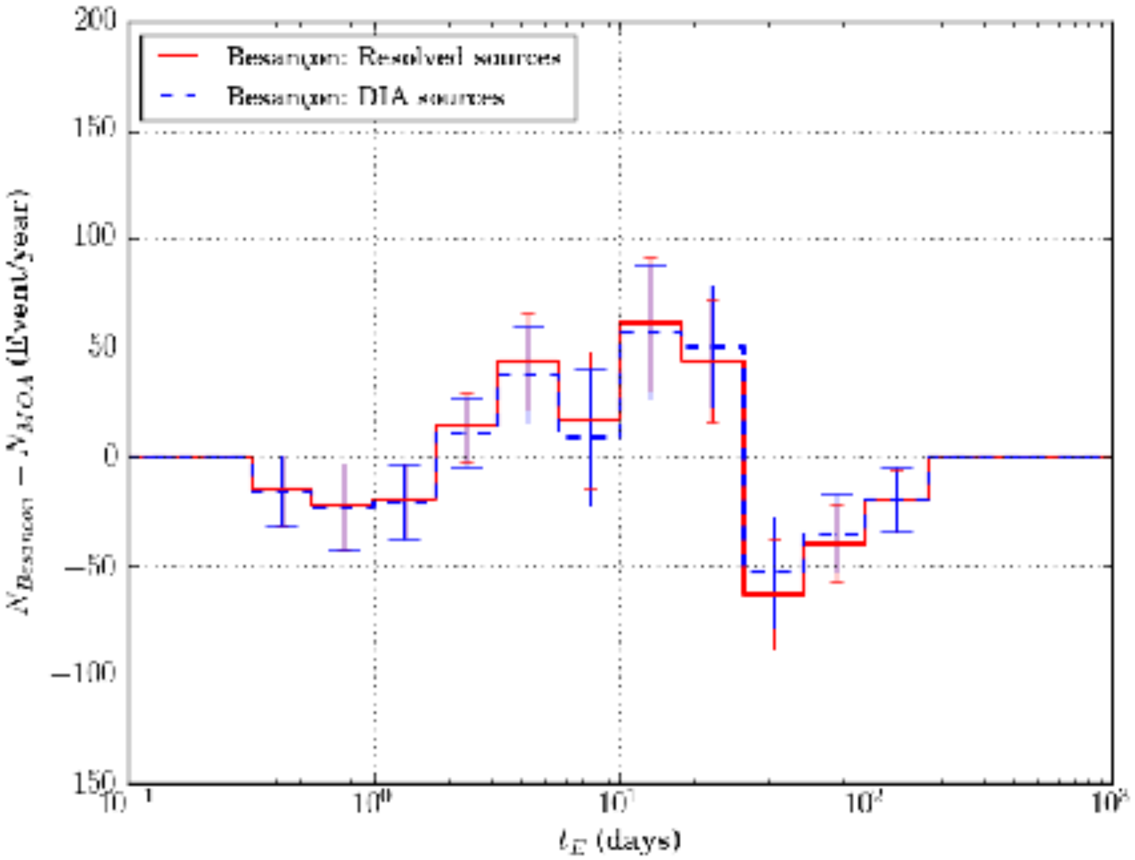

Figure 3. The Einstein radius crossing time distribution of the MOA-II survey, OGLE-III events in $-2^\circ < l < 2^\circ$ fields and the Besancon data with added low-mass stars and brown dwarfs (top) and the scaled residual between the MOA-II survey and the Besancon rates (bottom).

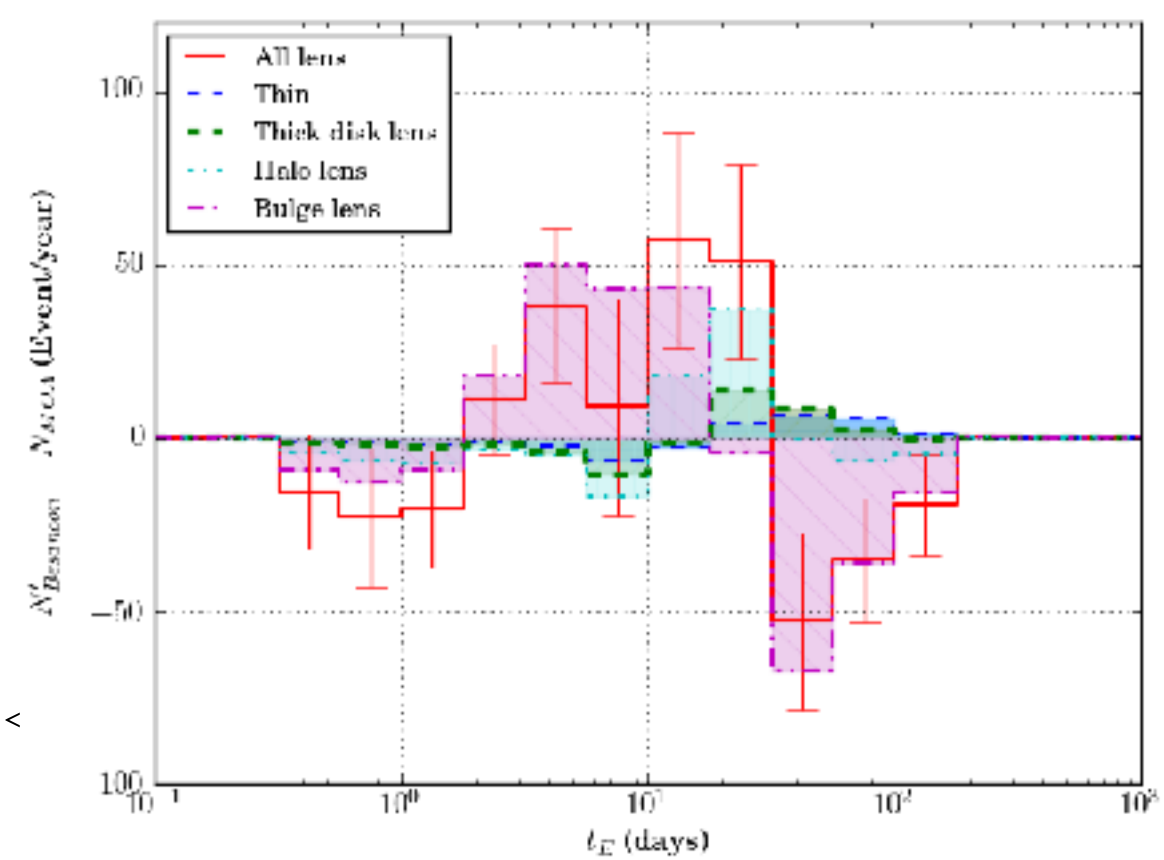

Event time scale

- $t_E = \theta_E / \mu$
- The bar pattern speed (factor of 2 uncertainty) impacts the relative proper motion for disc/bulge events, or for foreground bulge/background bulge events.
- A modified dynamical model could solve the problem (?)
- Conversely the distribution of event time scale could constrain the dynamics of the bar

Revised MOA optical depth
corrected for incompleteness in star counts on the RC

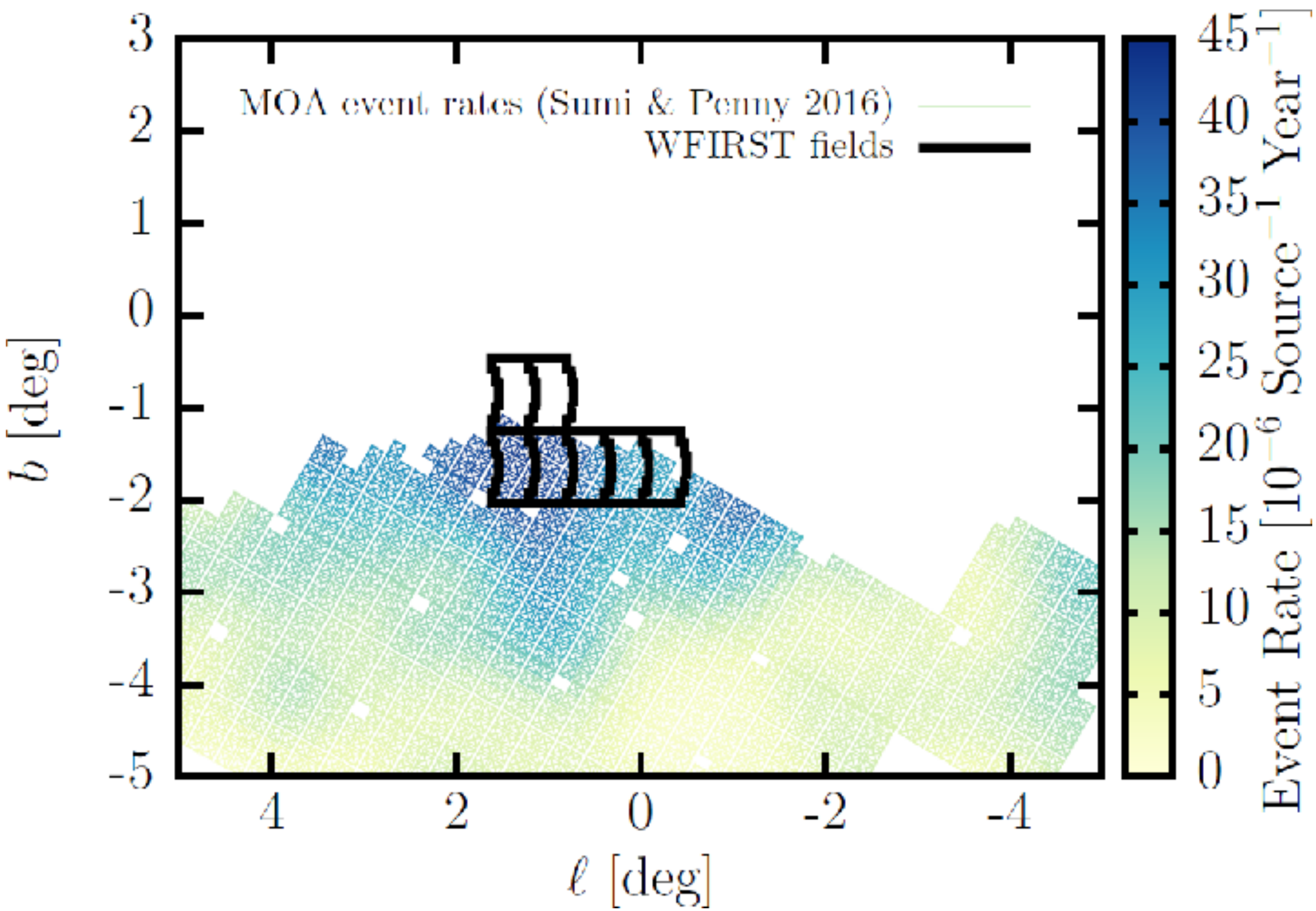

2016ApJ...827..139S

Courtesy M. Penny

Revised optical depth in MOA compared with Besançon model 2011

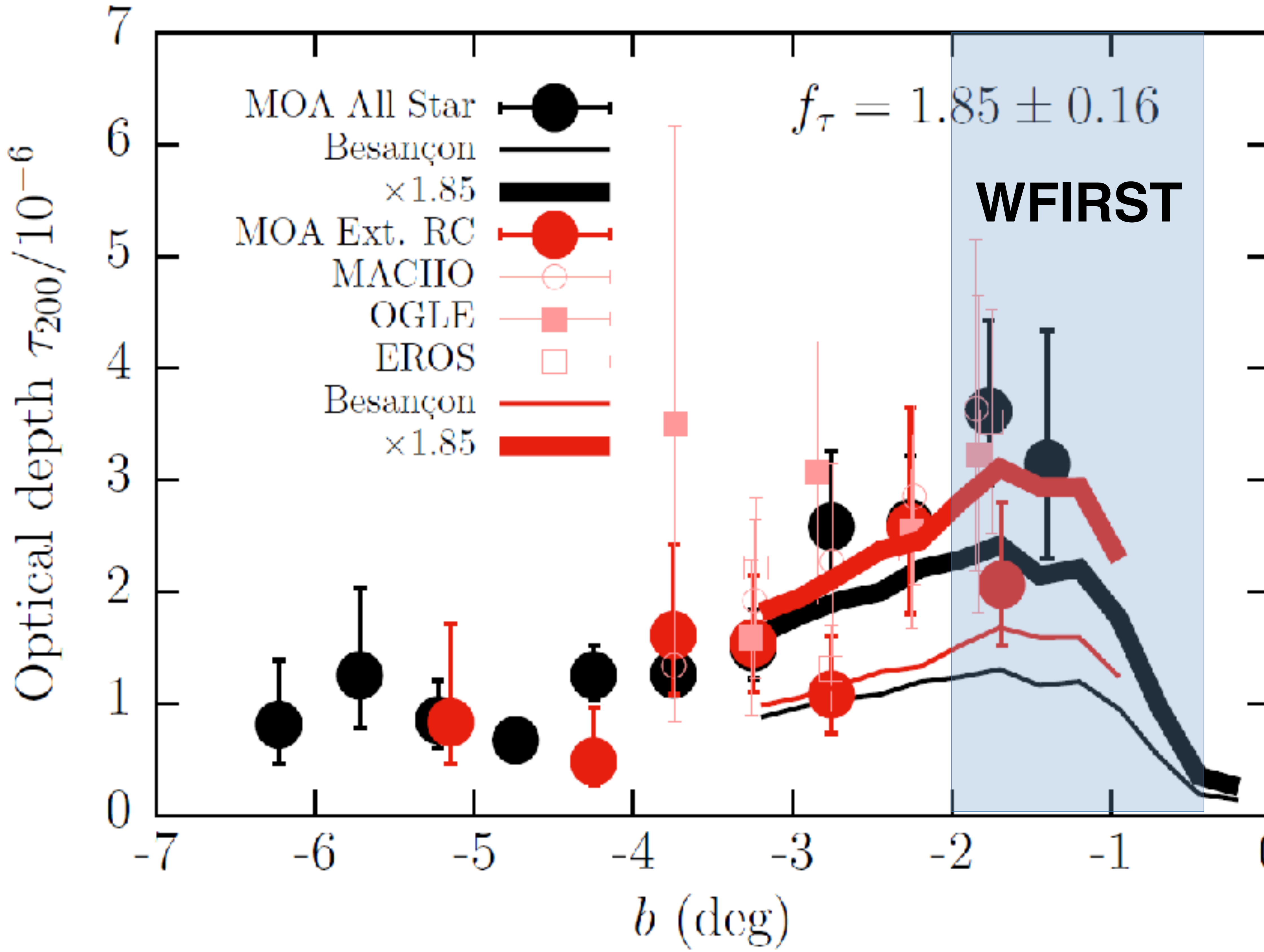

Need correction factor at b>-3°

Courtesy M. Penny

Revised event rate in MOA compared with Besançon model 2011

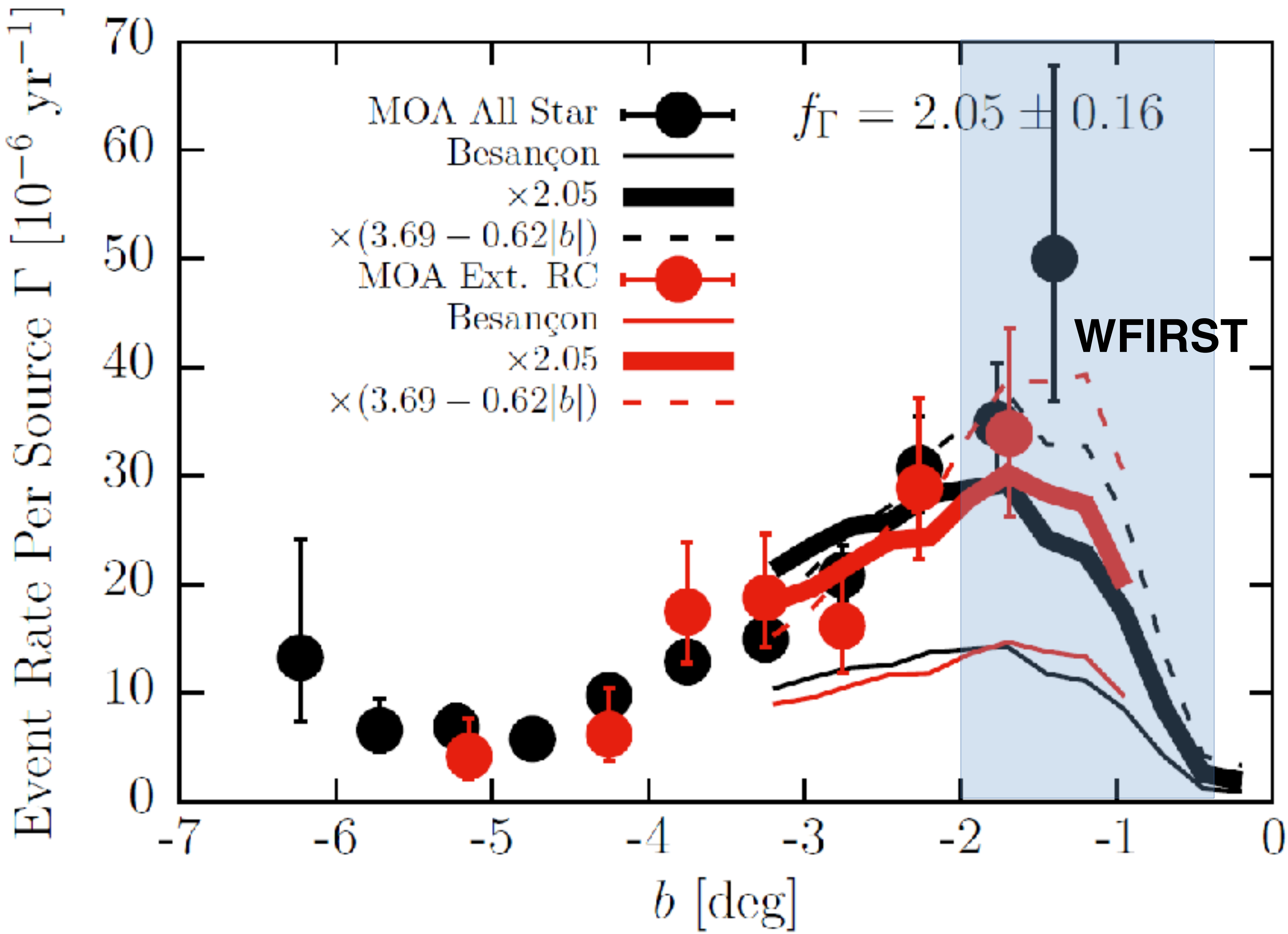

Courtesy M. Penny

Revised optical depth as a fct of latitude compared with BGM 2013

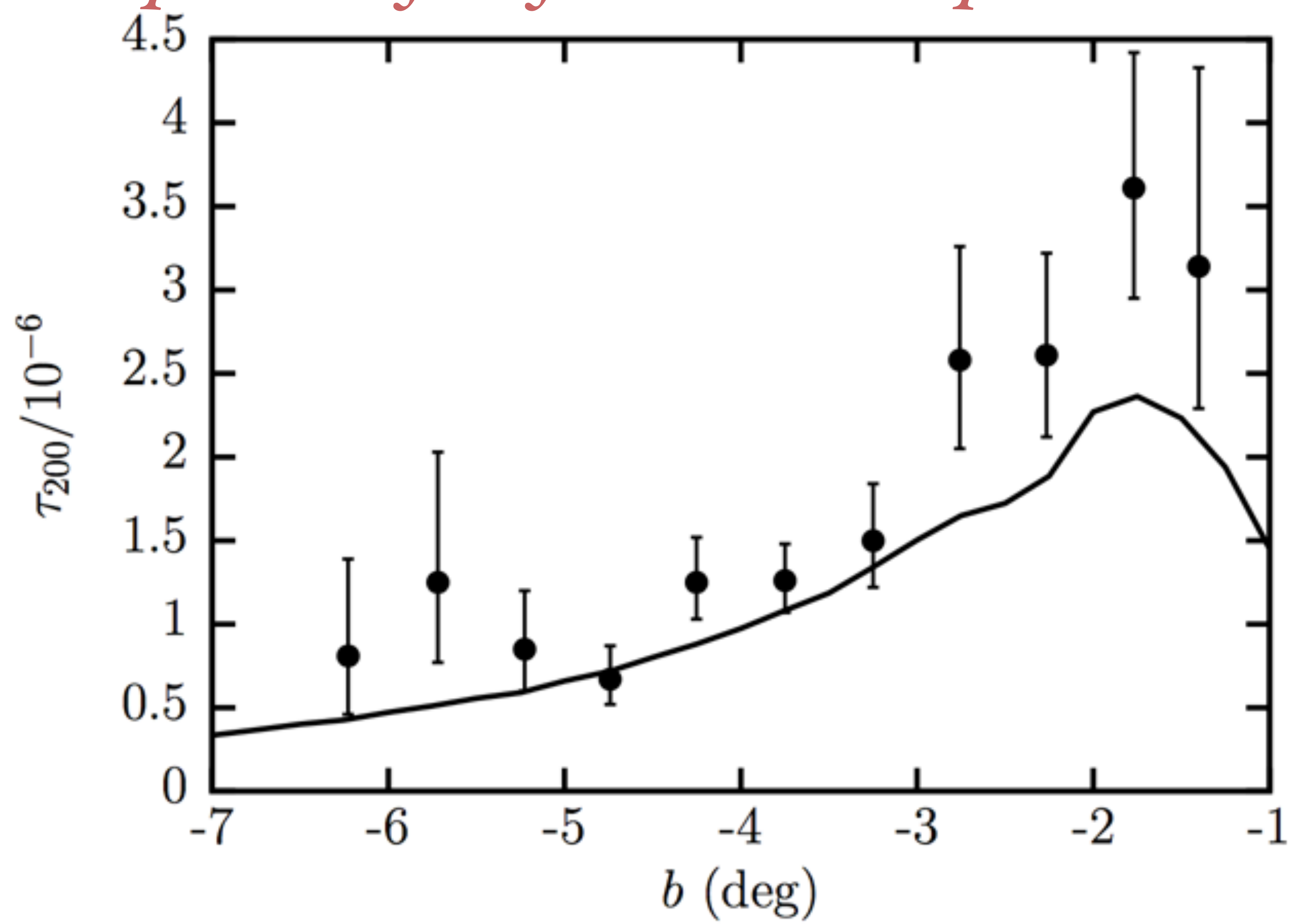

Fig. 14.—: The optical depth for events with $t_E < 200$ days, τ_{200}, for the all-source sample as a function of the galactic latitude b (filled circles with error bars), and the theoretical model from the Besançon model by Awiphan, Kerins & Robin (2016) (solid line). It is better agreement than the original τ measurements by Sumi et al. (2013), while they are still slightly higher.

Smaller discrepancy

Sumi & Penny, 2016

Event rate per star per year as a fct of latitude

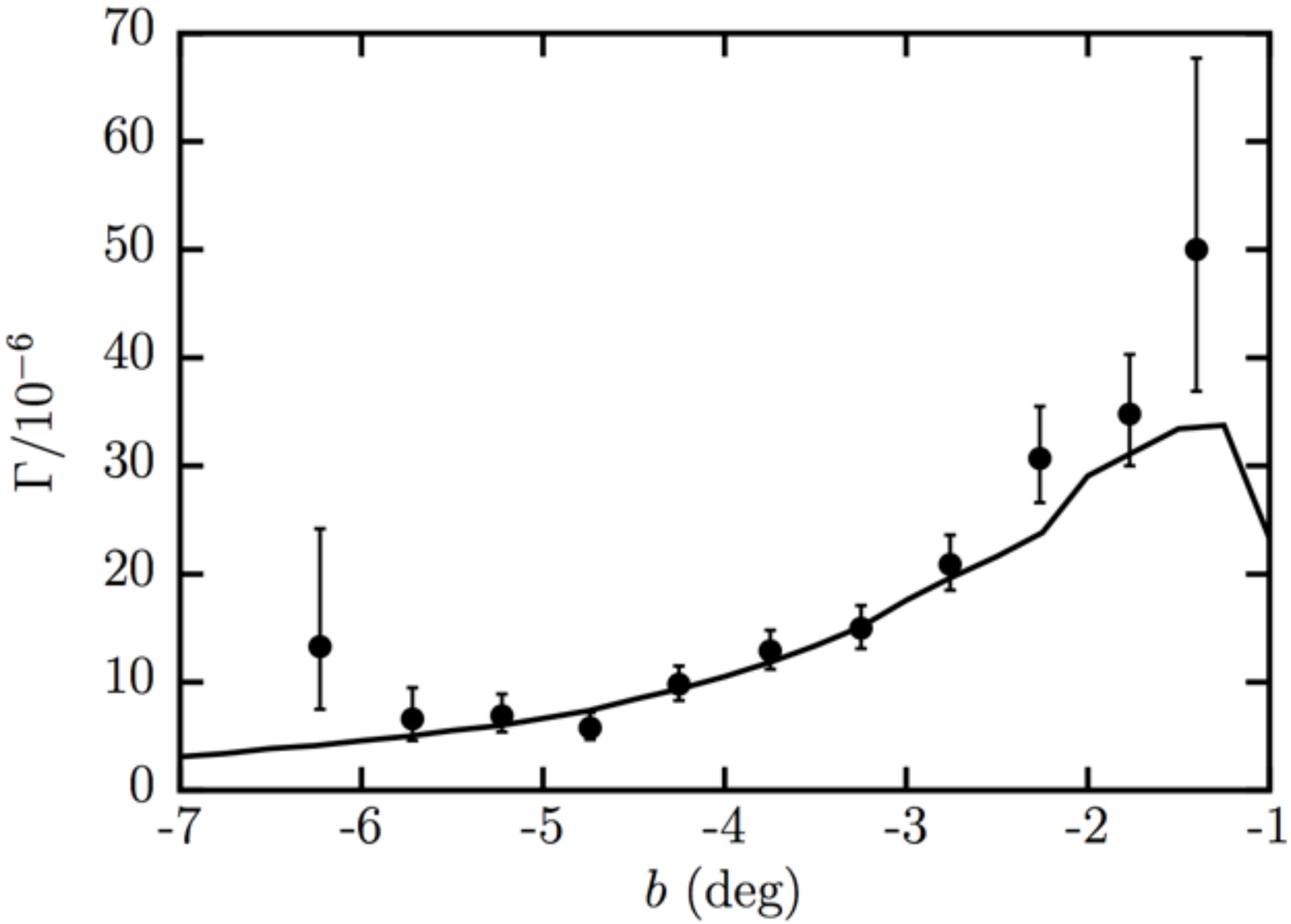

Fig. 15.—: The event rate per star per year, Γ, for the all-source sample as a function of the galactic latitude b (filled circles with error bars), and the theoretical model from the Besançon model by Awiphan, Kerins & Robin (2016) (solid line). They are consistent.

Consistent but still lower at b>-2.5°

Sumi & Penny, 2016

Inner bulge/bar

- Missing inner bar/bulge (Robin et al, 2012, Wegg & Gerhard 2013)

Residuals 2MASS-BGM star counts

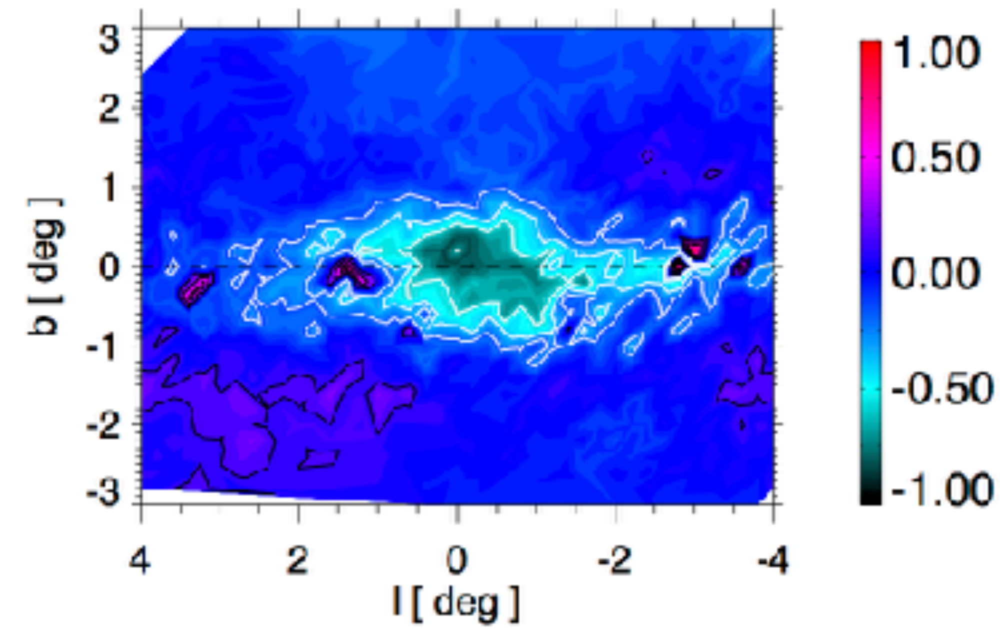

- Extra component in Simion et al, 2017

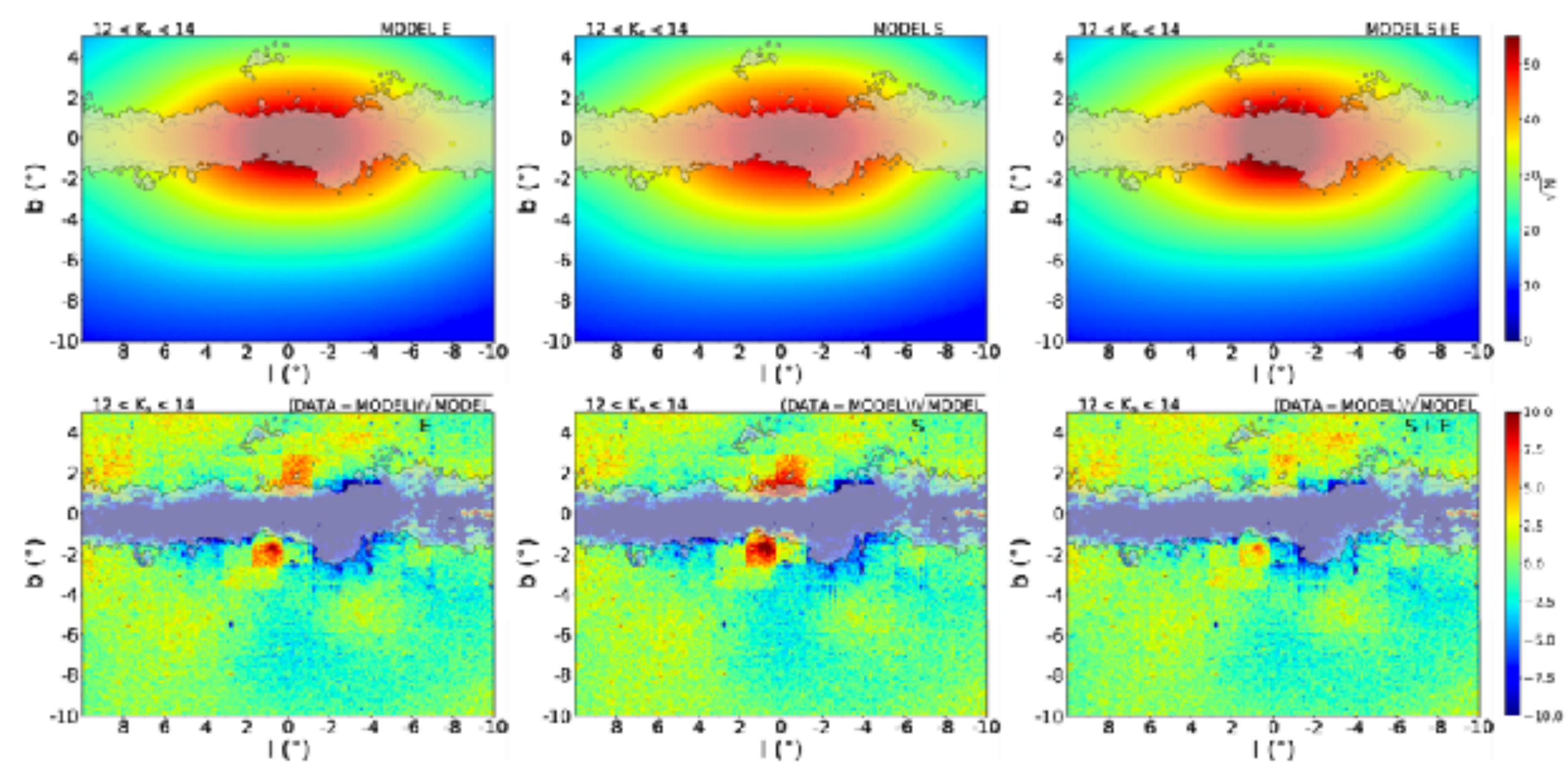

Nuclear region

- Disky pseudo-bulge
- Nuclear bar
- Probably young
- Simion: S+E model fit : bar shaped (1.47, 0.24, 0.26), angle -2° (end-on), young (bright Red clump)

Nuclear component E | *Residuals without E* | *Residuals with E*

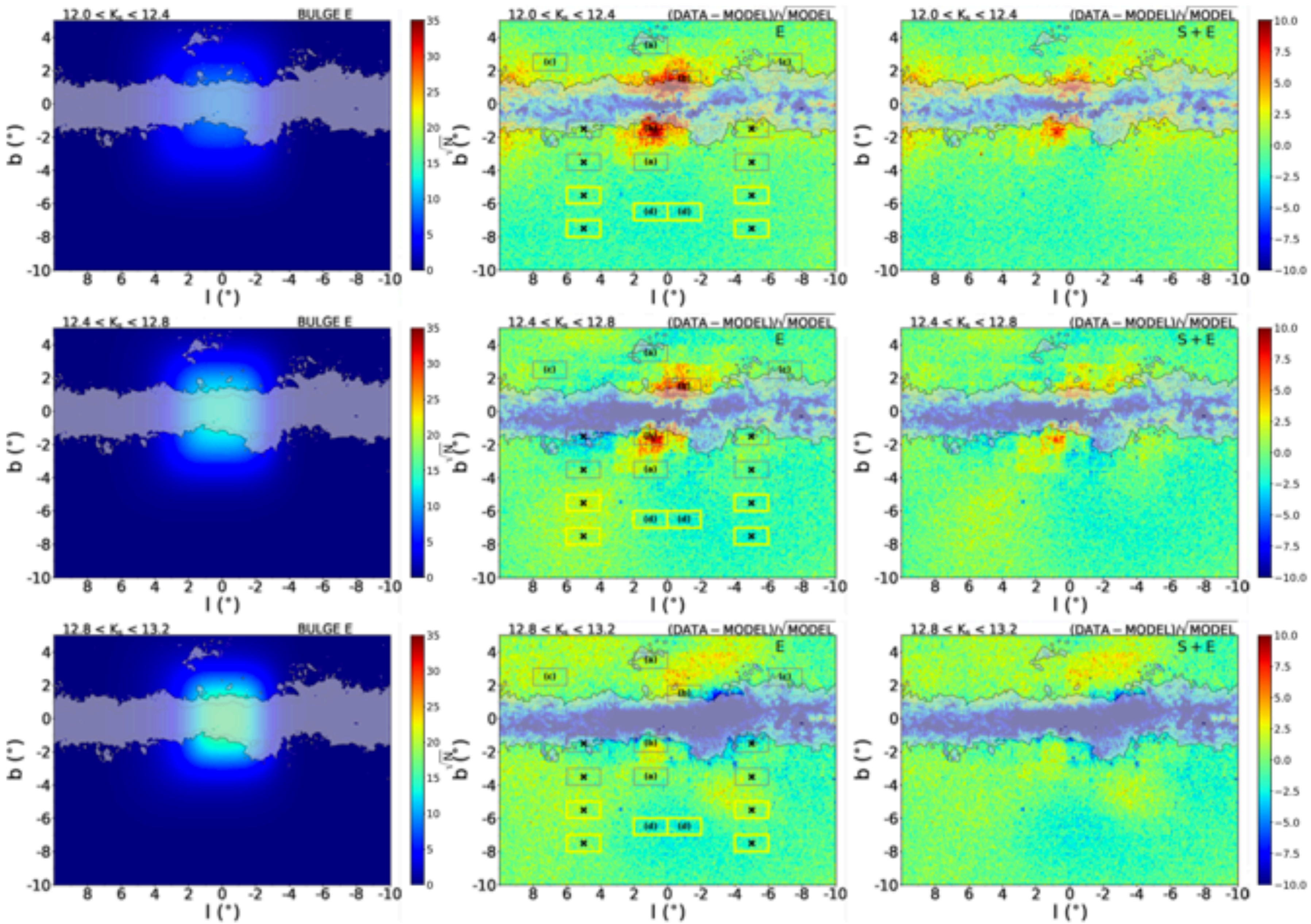

Summary microlensing comparisons

- Overall agreement between predictions and data, although BGM might underestimate the rates at b~-2°.
- Can be solved with a nuclear bar or disk population (to be confirmed)
- Uncertainties of optical depth due to incompleteness (efficiency of detection estimate)
- Uncertainties in models on the bulge mass, dynamics
- Different models can explain the observed optical depth and event rate
- Extrapolation to estimate microlensing in WFIRST

Exoplanets from microlensing

- BGM predictions (Ban et al, 2016) for Euclid and WFIRST free floating planets
- Use updated BGM2012 (wrt Penny et al, 2013), corrected by a factor 1.6

FFP (Ban et al 2016)

WFIRST

Table 3. The maximuml values and area integrated FFP event rates in SN mode for 100% detection efficiency and assuming $u_{max} = 1$.

Lens mass		I-band (ground)	K-band (ground)	H-band (space)
	max	3700	15 000	26 000
Stellar	location	(0°.75, −1°.75)	(1°, −0°.75)	(0°.25, 0°.25)
	global	58 000	450 000	710, 000
	max	200 [−0.3%]	850 [0.4%]	1500 [1.4%]
Jupiter	location	(0°.75, −1°.75)	(1°, −0°.75)	(−1°.50, 0°)
	global	3100	25 000	40 000
	max	36 [1.6%]	170 [−6.5%]	340 [0.05%]
Neptune	location	(0°.75, −1°.75)	(1°, −0°.75)	(−1°.50, 0°)
	global	460	4900	8900
	max	1.1 [−22%]	12 [−20%]	68 [−4.9%]
Earth	location	(0°.25, −2°)	(1°, −1°.50)	(−1°.50, 0°.50)
	global	18	350	2000

Notes. The maximum rates are in units of events yr^{-1} deg^{-2} with the rate contrast in square brackets for FFPs. The hot-spot location is given in the Galactic coordinates (l, b). The global rates are in units of events yr^{-1} which covers the whole simulation area of 200 deg^2. The errors of these maximum rates are all <1%, and a correction factor of 1.6 has been applied to the rate.

Ban et al, 2016: estimated event rate

Estimated event rate for earth mass planets

- Ground based I band
- Ground based K band
- Space based H band

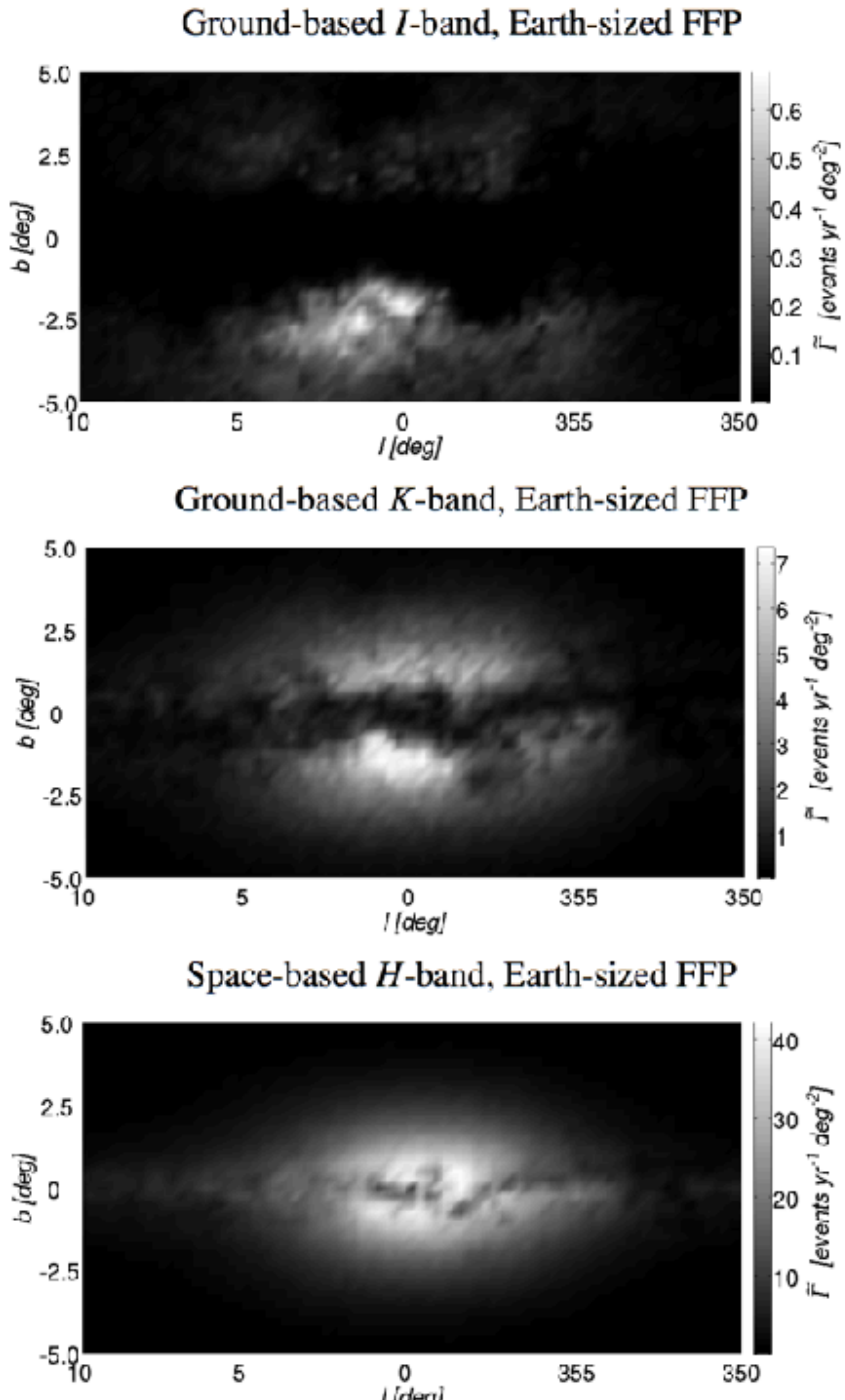

Ban et al (2016)

Estimated event time scale for earth mass planets

- Ground based I band
- Ground based K band
- Space based H band

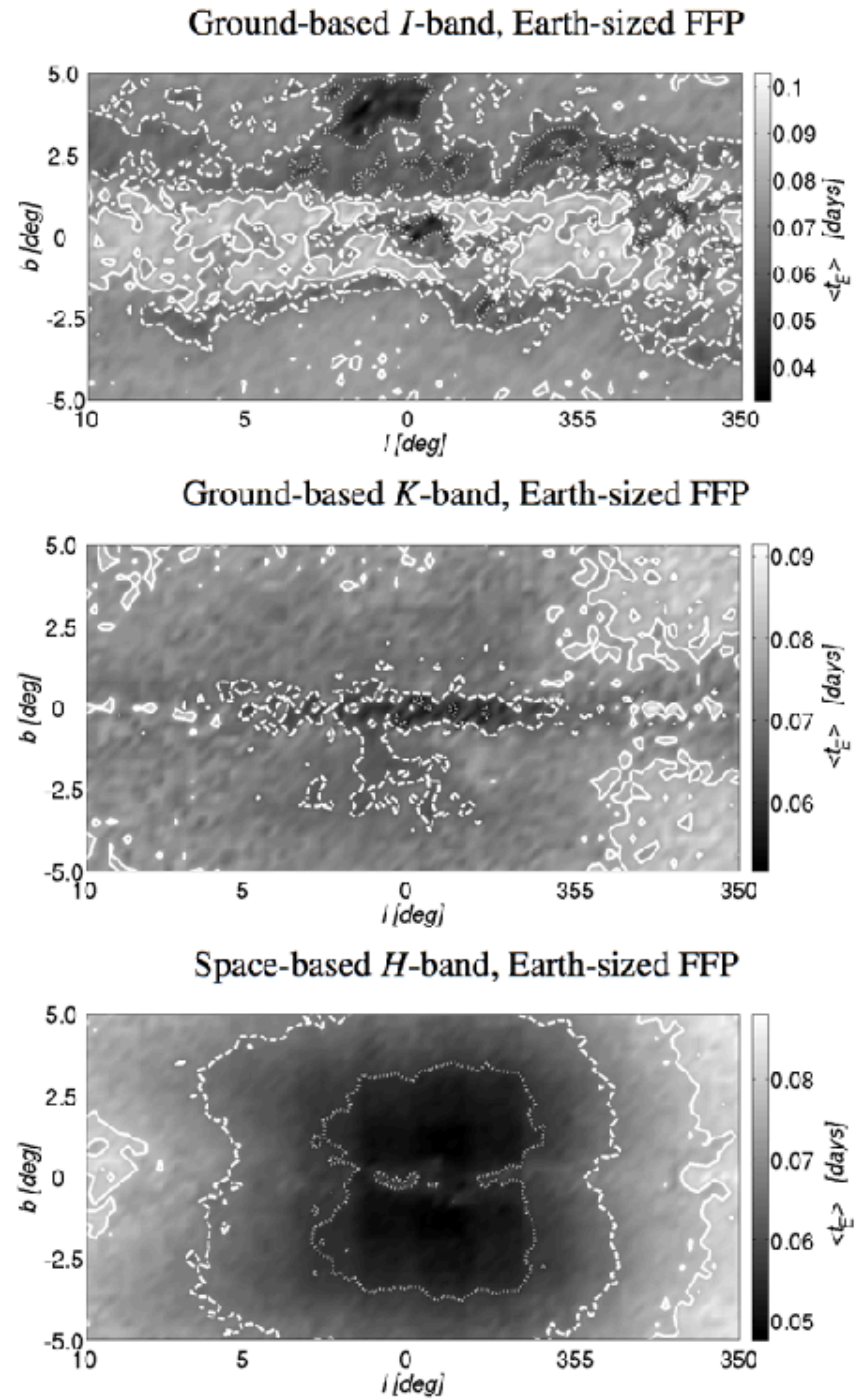

Bulge archeology

- WFIRST 0.3% distances => shape and bar angle
- Ages (assuming good stellar models) : star formation histories, chemo-dynamics
- Classical bulge vs pseudo-bulge question, different populations (disk hole… nuclear bar… thick disk…)
- Very complementary to Gaia (distances accuracy ~10% in the bulge and only for bright stars)
- Microlensing: dwarf stars, Gaia: bright giants

Constraints on dark matter distribution

- Wegg, Gerhard & Portail (2016) : constraints on dark matter : range of baryonic rotation curves compatible with MOA-II data

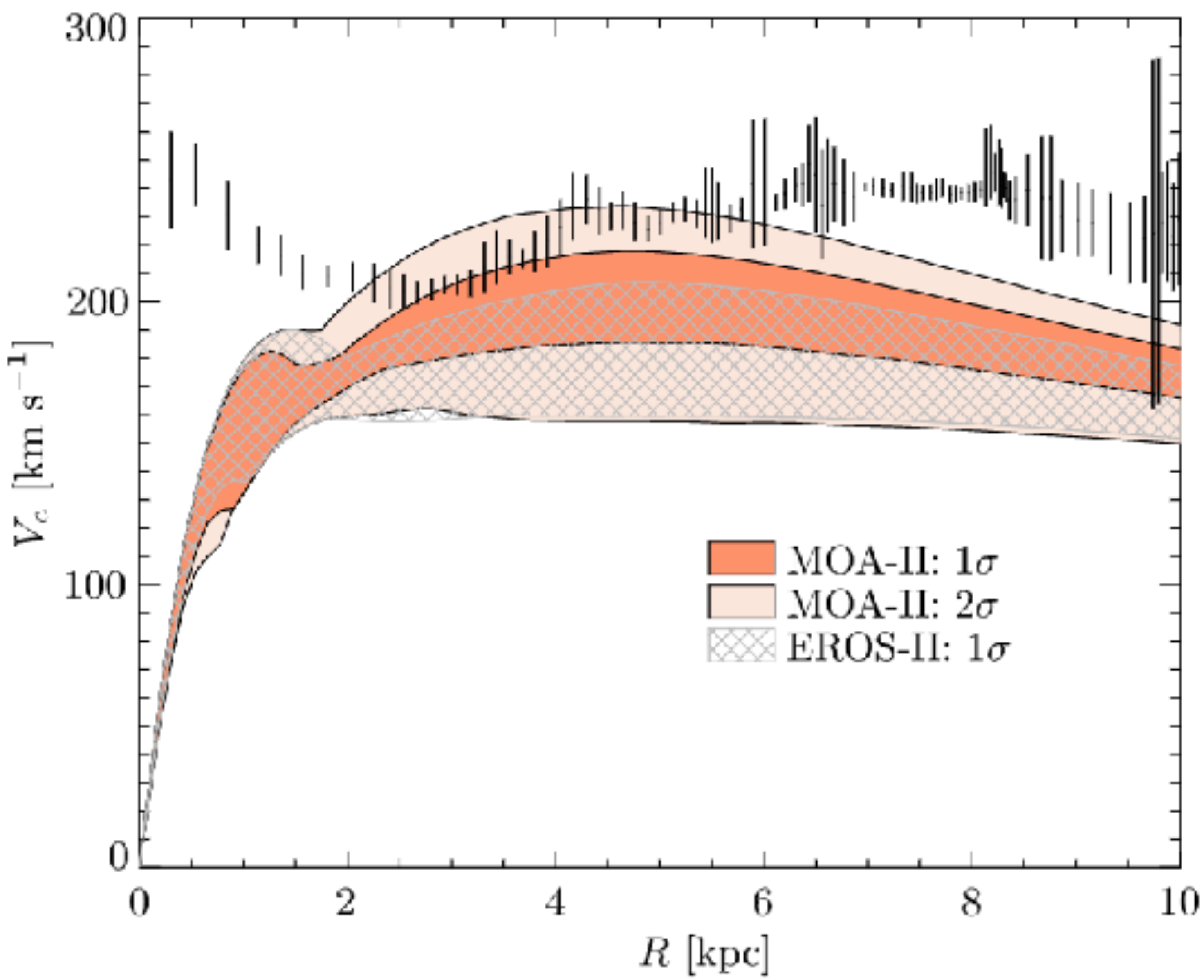

- Low dark matter content in the inner Galaxy
- Near maximum disk

Constraints on the IMF from microlensing

- Wegg, Gerhard & Portail (2017): constraints on the IMF

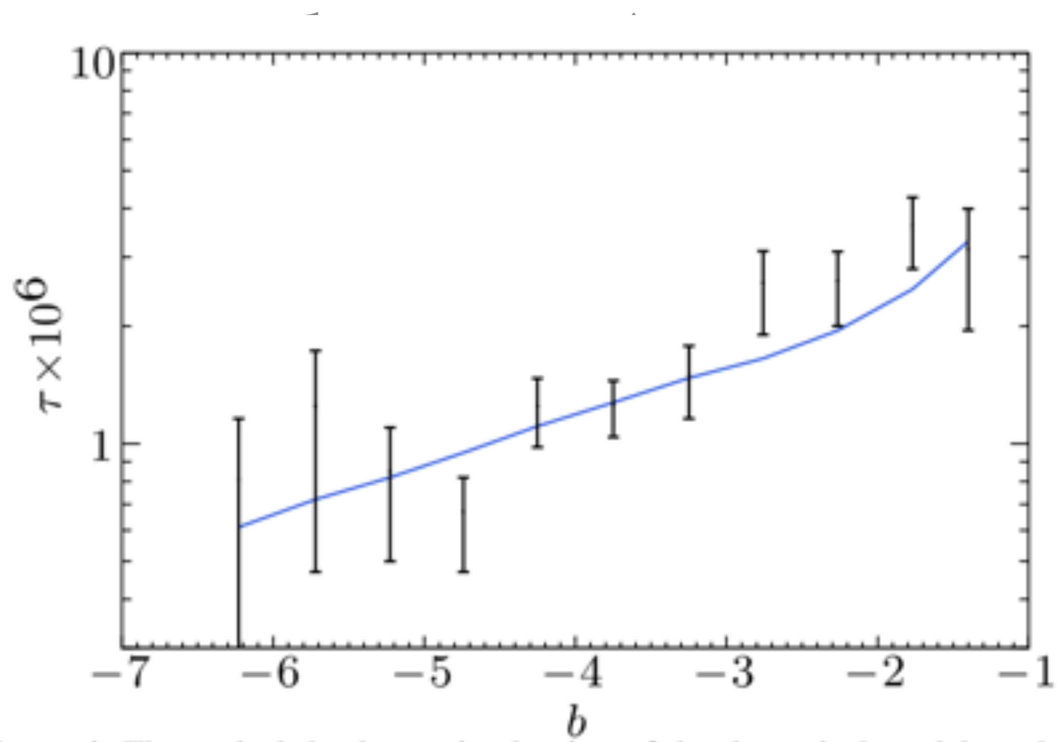

Figure 1. The optical depth to microlensing of the dynamical model used in this work. Upper panel: optical depth averaged over stars with an unextincted source magnitude $14 < I_s < 19$. Lower panel: comparison with the optical depths measured by Sumi & Penny (2016). Both panels use the methods outlined in Wegg et al. (2016), with the updated dynamical model of P17.

- IMF : similar to the local disk

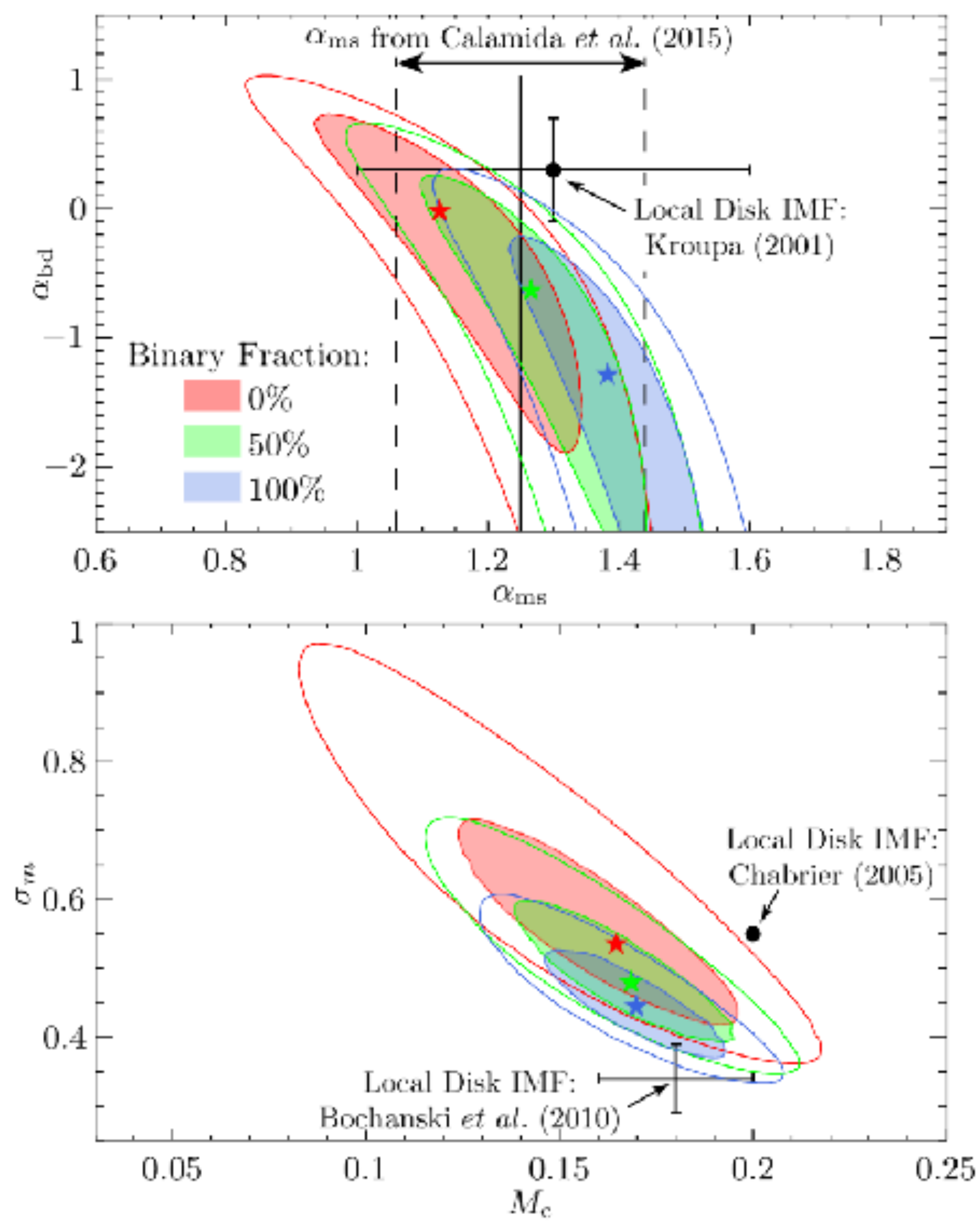

Effect on the time distribution of the stellar IMF

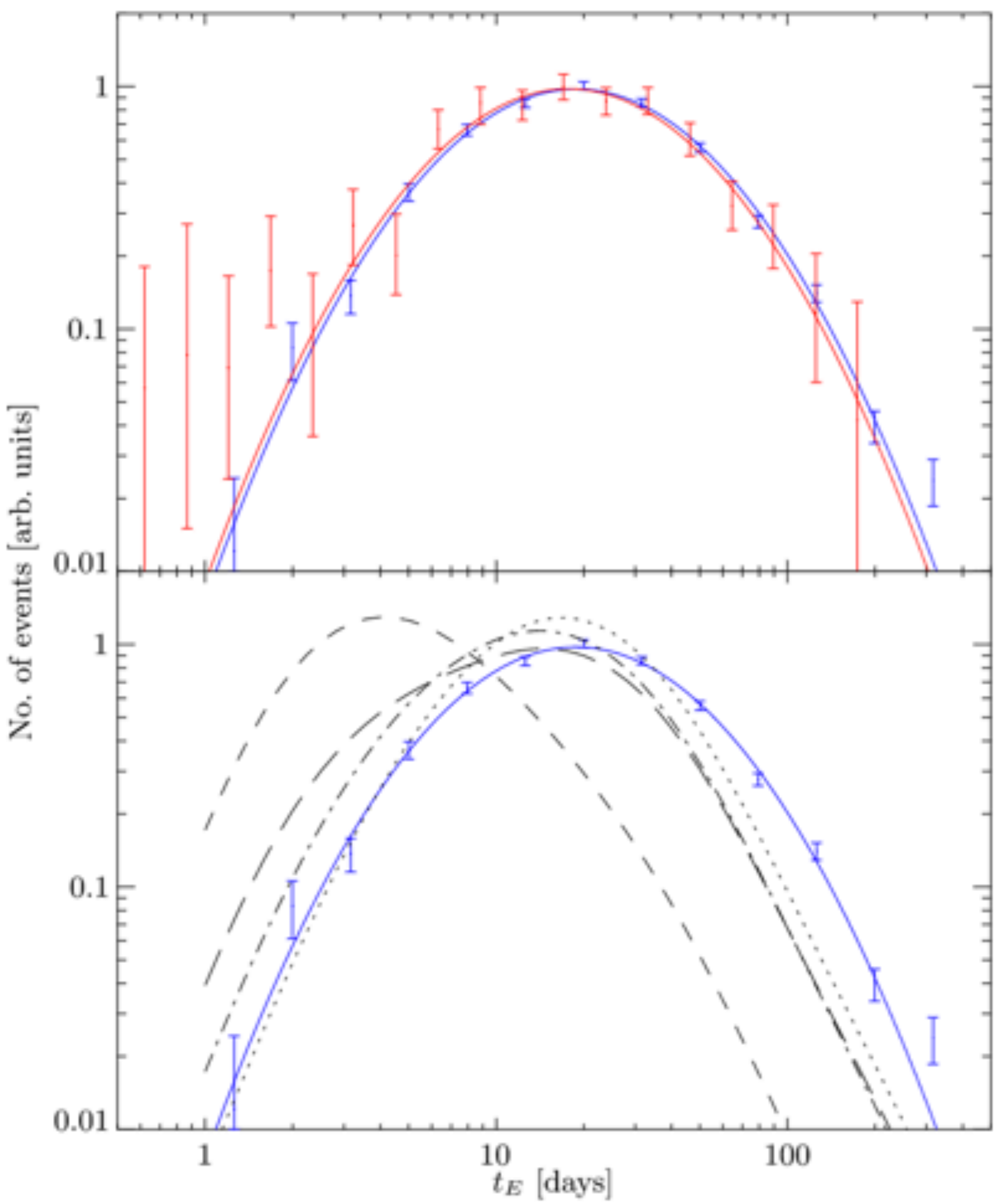

Red: MOA-II
Blue: OGLE-III

Model IMF:

Salpeter 1955 1 slope power law
Zoccali+2000
Kroupa+2001 2 slope power law
Calamida+2015 log-normal

Wegg, Gerhard & Portail (2017) 2017ApJ...843L...5W

Conclusions

- Galaxy Models can be used to estimate the micro-lensing rate for WFIRST and other future space missions
- Conversely, results from these missions will constrain our knowledge of Galactic structure, kinematics, and planet populations
- Use the tool: http://www.mabuls.net
- Need to be updated with a more recent Galaxy model (2016-2017)

http://www.mabuls.net

Manchester-Besançon Microlensing Simulator

(MaBμlS)

Description | Changelog | Terms of use

Besancon version: (•) 1307

Filter: I band

Source selection: (•) Resolved sources ( ) DIA sources

Bright magnitude limit: [ ]

Min	Property	Max
-10.125	Galactic longitude (°)	9.875
-9.875	Galactic latitude (°)	10.125
-1	Apparent magnitude	19
1.0	Event duration (t_E/days)	1000.0

Lens population: (•) All ( ) Disk ( ) Bulge

Microlensing property:
- (•) Optical depth
- ( ) Average Einstein radius crossing time
- ( ) Event rate per sky area
- ( ) Event rate per source star

Microlensing map image parameters

Interpolation: (•) Nearest neighbour ( ) Bilinear

Contours: [ ] 0 No. of contours

Colour bar stretch power law: [ ] 1 Power

Intensity clipping: [ ] 100 Percentile

Thanks for your attention